NACA RM L57D23

NACA

RESEARCH MEMORANDUM

HIGH-PRESSURE BLOWING OVER FLAP AND WING LEADING EDGE OF A THIN LARGE-SCALE 49° SWEPT WING-BODY-TAIL CONFIGURATION IN COMBINATION WITH A DROOPED NOSE AND A NOSE WITH A RADIUS INCREASE

By Marvin P. Fink and H. Clyde McLemore

Langley Aeronautical Laboratory
Langley Field, Va.

NATIONAL ADVISORY COMMITTEE FOR AERONAUTICS

WASHINGTON
May 28, 1957
Declassified September 17, 1958

NACA RM L57D23

NATIONAL ADVISORY COMMITTEE FOR AERONAUTICS

RESEARCH MEMORANDUM

HIGH-PRESSURE BLOWING OVER FLAP AND WING LEADING EDGE OF A THIN LARGE-SCALE 49° SWEPT WING-BODY-TAIL CONFIGURATION IN COMBINATION WITH A DROOPED NOSE AND A NOSE WITH A RADIUS INCREASE

By Marvin P. Fink and H. Clyde McLemore

SUMMARY

A 49° swept-wing complete model equipped for high-pressure blowing full span at two chordwise locations at the leading edge of a full-span wing and over a half-span flap has been tested in the Langley full-scale tunnel to determine the effectiveness of blowing at the leading edge as a supplementary leading-edge stall control at high lift coefficients.

The wing had 49° of leading-edge sweep, an aspect ratio of 3.5, a taper ratio of 0.3, and an NACA 65A006 airfoil parallel to the plane of symmetry. Lift, drag, and pitching-moment data were taken over an angle-of-attack range from -4° to 28° for the model with blowing applied to the trailing-edge flap and to the wing leading edge in combination with leading-edge-droop and leading-edge-radius modifications. The tests were conducted at a Reynolds number of 5.2×10^6 and a Mach number of 0.08.

The results show that neither leading-edge droop nor leading-edge-radius increase was an adequate leading-edge stall-control device when used in conjunction with an effective boundary-layer-control flap configuration. However, blowing applied near the wing leading edge improved the stall-control ability of both the drooped nose and the nose with a radius increase and extended the angle-of-attack range and maximum lift coefficient appreciably. Because of the mechanical difficulty of constructing a nose slot sufficiently forward on thin wings to control flow separation at the leading edge, blowing at the nose alone was ineffective for the basic airfoil section. The addition of droop or radius increase

was required in order to achieve effective stall control. For the drooped-nose configuration, blowing from either the slot at the knee of the droop or the slot located on the upper surface near the leading edge produced similar gains in lift.

Blowing at the leading edge of the wing for either nose droop or radius increase produced little change in pitching moment at a given lift coefficient below maximum lift coefficient. The pitching-moment curves were substantially linear up to maximum lift coefficient with a slight pitch-up characteristic at stall. The investigation indicates that the application of boundary-layer control should result in appreciable reductions in landing approach and touchdown speeds for an airplane of this configuration.

INTRODUCTION

The need for increased lift capabilities of thin low-aspect-ratio wings resulting from ever-increasing wing loadings has led to considerable research on methods for attaining more lift on currently used wing geometric characteristics. Literature reporting the results of investigations along this line shows that boundary-layer control applied to a trailing-edge flap can produce appreciable incremental lift increases. However, if this greater flap effectiveness is to be exploited to the fullest on wings with thin airfoil sections, a more effective leading-edge stall-control system than is now used with conventional trailing-edge flaps must be employed. The deficiency of devices such as the slat, drooped nose, and cambered leading edge, when used with a boundary-layer control flap (refs. 1, 2, and 3), is usually indicated by the moderate angle of attack at which maximum lift occurs. The cause of this leading-edge flow breakdown is the additional angle-of-attack type of loading associated with the more powerful trailing-edge-flap configuration.

In a previous study of the leading-edge stall-control problem (ref. 1), the need for using full-span devices on a thin swept wing equipped with trailing-edge-flap boundary-layer control was demonstrated, and limited tests utilizing blowing from a slot near the wing leading edge suggested the possibility of combining blowing with leading-edge droop or leading-edge camber and radius increase to provide effective stall control. Consequently, the model of reference 1 was modified to incorporate a full-span leading-edge drooped nose of 0.17 chord with blowing slots provided to allow air to be ejected either from a slot near the airfoil nose or from a slot at the knee of the drooped nose.

The present report presents the results of tests to determine the effectiveness of leading-edge stall control of blowing near the wing leading edge in combination with leading-edge droop and leading-edge

radius modifications for a range of trailing-edge-flap blowing conditions. The range of blowing flow rates for these tests was selected primarily to represent the quantities of air compatible with the compressor air-bleed limits of current turbojet engines. A few tests were conducted, however, with flow rates representative of those associated with an auxiliary engine exhaust system.

The model used in this investigation was a large-scale boundary-layer control configuration complete with wing, body, and tail. The wing was swept back 49° at the leading edge and had an aspect ratio of 3.5, a taper ratio of 0.3, and an NACA 65A006 airfoil section.

Tests of this investigation were conducted in the Langley full-scale tunnel for a range of angle of attack from -4° to 28° at a Reynolds number of 5.2×10^6 and a Mach number of 0.08.

COEFFICIENTS AND SYMBOLS

C_L lift coefficient, $\frac{\text{Lift}}{q_\infty S}$

$\Delta C_{L,\alpha=0^\circ}$ increment in lift coefficient due to flap deflection at $\alpha = 0^\circ$

$C_{L,max}$ maximum lift coefficient

C_D drag coefficient (drag equivalent of pumping power not included), $\frac{\text{Drag}}{q_\infty S}$

C_m pitching-moment coefficient about $\bar{c}/4$ (see fig. 1), $\frac{\text{Pitching moment}}{q_\infty S\bar{c}}$

dC_m/dC_L rate of change of pitching-moment coefficient with lift coefficient

C_l rolling-moment coefficient, $\frac{\text{Rolling moment}}{q_\infty Sb}$

C_n yawing-moment coefficient, $\frac{\text{Yawing moment}}{q_\infty Sb}$

C_Q flow coefficient, $\frac{Q}{V_\infty S}$

C_μ momentum coefficient, $\frac{Q\rho_j V_j}{q_\infty S}$ or $\frac{GV_j}{gq_\infty S}$

q_∞ free-stream dynamic pressure, $\frac{1}{2}\rho_\infty V_\infty^2$

L/D lift-drag ratio

c local wing chord measured parallel to plane of symmetry, ft

$\bar{c}$ mean aerodynamic chord, $\frac{2}{S}\int_0^{b/2} c^2 dy$, ft

c_{av} average chord of wing measured parallel to plane of symmetry, S/b, ft

b wing span, ft

y spanwise distance measured perpendicular to plane of symmetry, ft

S area of wing, sq ft

R Reynolds number based on mean aerodynamic chord

V velocity of flight, knots

V_∞ free-stream velocity, ft/sec

V_j velocity of ejected air at slot, ft/sec

ρ_∞ mass density of free-stream air, slugs/cu ft

ρ_j mass density of ejected air at slot, slugs/cu ft

Q volume of flow of air blown out of slot, cu ft/sec

G weight of flow of air from slot, lb/sec

g acceleration due to gravity, ft/sec^2

α angle of attack, deg

δ flap deflection (relative to wing chord plane) measured perpendicular to flap hinge line, deg

T thrust, lb

$\bar{c}_t$ mean aerodynamic chord of horizontal tail

I inboard boundary-layer control compartment

C center boundary-layer control compartment

O outboard boundary-layer control compartment

Subscripts and abbreviations:

f flap

LE wing leading edge

TE wing trailing edge

BLC boundary-layer control

APPARATUS AND TESTS

Model

The model for the investigation was a large-scale complete model equipped for a high-pressure leading- and trailing-edge blowing type of boundary-layer control. The general layout and principal dimensions of the model are given in figure 1, and a photograph of the model mounted for testing is given in figure 2. The wing had an area of 224 square feet, 49° of sweep at the leading edge, an aspect ratio of 3.5, a taper ratio of 0.3, and NACA 65A006 airfoil sections parallel to the plane of symmetry. An 0.24c half-span plain trailing-edge flap employing a wing-shroud blowing jet (see fig. 3) was used as a high-lift device.

Two of the wing leading-edge flow-control devices used for the tests were full span. One was an 0.17c drooped nose hinged at the lower surface of the wing. The other control device was the 0.013c radius increase of the nose which was added in a manner to provide a cambered leading edge. Blowing air was ejected at the forward part of the wing from one or the other of the two slots indicated in figure 3. The more forward slot (called the nose slot) was constructed as close to the leading edge of the wing as possible and yet still have the issuing jet adhere to the wing surface. The nose slot was, therefore, about 0.5 inch behind the leading edge from the wing tip to the root. The rear leading-edge slot (called the knee slot) was located so that it would be ahead of any great contour change caused by deflecting the nose. Consequently, the blowing jet would be ahead of the separation point. As the nose was deflected, the knee slot became exposed at an angle of 20°.

The nose-slot ramp angle was determined from preliminary bench tests to ascertain that, for the pressure ratios to be used during the wind-tunnel tests, the jet of air from the slot would negotiate the curvature of the rear-slot lip and remain attached to the wing surface. For the conditions of slot geometric characteristics and pressure ratios employed on this configuration, it was found that the ramp angle (as measured between a feeler gage inserted in the slot and a mean tangent line) could not be more than about 40°.

The nose droop, which could be deflected to an angle of 50° normal to the hinge line, was divided into three spanwise compartments (fig. 1) - inboard (0.324b/2), center (0.203b/2), and outboard (0.331b/2) - and is referred to hereinafter as I, C, and O, respectively, for blowing over either the nose or knee. The leading-edge blowing air was supplied from one main duct within the wing and for experimental purposes was valved to each of the six individual leading-edge compartments.

All the blowing slots were adjustable so that mass flow could be regulated by slot area or individual compartment pressure. For most of the tests, all slots were maintained at a gap setting of 0.010 inch. The trailing-edge-flap blowing slot, however, was set at a 0.050-inch gap for flap mass-flow coefficients $C_{\mu,f}$ greater than 0.10. Typical cross-sectional views of leading- and trailing-edge slots are shown in figure 3.

Air Supply

The air used for boundary-layer control was supplied by a compressor capable of delivering to the model at full flow and at a pressure ratio of 3.0 a maximum of air about 12 pounds per second. The compressor was isolated from the model, and air was delivered to the model through a system of ducting. The air was brought onto the scale-balance frame supporting the model by flexible connections alined so that reaction forces would cancel each other. In order to permit angle-of-attack change, there was located within the model on the lateral axis of rotation an air-tight slip joint between the wing plenum and the air-supply pipe entering the model through the bottom of the fuselage.

Method

The mass flow of air being ejected from the individual blowing slots was calculated from the individual duct pressure, temperature measurements, and the slot-exit area. The results from this method, checked in another investigation, are comparable in accuracy to the results obtained from measuring the flow through a standard orifice plate.

Several shielded total-pressure tubes were located within each slot plenum chamber to ascertain that uniform flow was achieved along the length of the slot. Duct pressure was indicated by a mercury manometer; duct temperature, by a thermocouple. Slot areas were measured with test pressure applied.

Tests

The force data, taken on the tunnel six-component scale-balance system, was measured over the angle-of-attack range from -4° to 28° at a Reynolds number of 5.2×10^6 which corresponds to a Mach number of 0.08.

Flap-effectiveness tests were made for the various leading-edge configurations for the conditions of no boundary-layer control and with blowing over the flap. The flap-effectiveness tests with blowing over the flap covered a range of flap deflections up to 60° and momentum coefficients C_μ up to 0.18. From these results several momentum coefficients with blowing over the trailing-edge flap, representing minimum, moderate, and fairly high momentum coefficients ($C_{\mu,f}$ = 0.01, 0.03, and 0.10, respectively), were chosen for flap conditions for the tests of the leading-edge control devices (droop and radius increase) with blowing applied over the leading edge.

The test conditions with blowing over the leading edge include a variation of spanwise application of boundary-layer control by blowing from compartments I, C, and O at the nose and the knee-slot locations for the drooped-nose configuration. However, only nose-slot blowing was tested for the radius-increase configuration.

Variation of blowing rates from one spanwise compartment to the other was also investigated by varying the air pressure within the individual compartments.

Corrections

The data have been corrected for airstream misalinement, buoyancy, and jet boundary effects. In order to make the present data equivalent to a self-contained system, the drag coefficients were corrected by adding the term $\rho Q V_\infty$ which is the drag equivalent of taking on board the mass of air ρQ that had an original velocity, relative to the model, of V_∞. This correction was necessary because the air ejected from the model was admitted from a source that actually had a zero component of momentum in the stream direction. The lift and drag data, as presented, contain the effects of the jet momentum because this would be reflected in the aerodynamic characteristics of a boundary-layer-control airplane.

RESULTS AND DISCUSSION

Lift Characteristics

Effect of flap deflection and flap boundary-layer control.- Since the results of an extensive investigation of the effect of boundary-layer control by blowing on a flapped-wing configuration have been reported in reference 1 only a small amount of data for the model with flaps deflected 40°, 50°, and 60° are presented for the condition without boundary-layer control (fig. 4). The results of tests with blowing over the flap are given in figure 5 for the flaps deflected 60° and for a range of momentum coefficients from 0 to 0.172. The incremental-lift gains obtained by boundary-layer control at zero angle of attack are summarized in figure 6. These data are in good agreement with the flap results of reference 1 and show that blowing continues to increase the lift for increases in blowing-momentum coefficient, although there is a considerable reduction in the rate of increase for C_μ values greater than 0.01 as noted by the change in slope in the curve of C_μ plotted against $\Delta C_{L,\alpha=0^\circ}$ (fig. 6). The point at which this change in slope occurs, generally referred to as the knee, usually indicates the minimum value of C_μ required to maintain unseparated flow on the flap for a given flap deflection and the most efficient use of the air available for boundary-layer control.

Effect of leading-edge droop.- The upwash at the leading edge of the highly loaded thin wings induced by the boundary-layer control flap caused early separation of the flow at the wing leading edge, and thus resulted in a large reduction of the stalling angle. In order to determine the effectiveness of droop as a leading-edge stall-control device on this model, the nose was drooped to 30°, 40°, and 45° for a flap deflection of 60° with no boundary-layer control applied. The results of these tests (fig. 7) show that stall at the leading edge was delayed. For the higher droop angles, tuft studies showed that separation finally occurred behind the knee and caused the wing tips to stall. A maximum lift coefficient of about 1.2 at $\alpha = 15^\circ$ was reached giving an incremental increase in lift coefficient of 0.2 over the basic leading-edge configuration. The expression "basic leading edge" refers to the original airfoil contour without any leading-edge modifications or blowing.

Inspection of figure 7 indicates that the application of just enough blowing to the 60° deflected flap for flow cleanup ($C_\mu \approx 0.01$) gave an appreciable lift-coefficient increase at low angles of attack for the clean leading-edge configuration but produced no appreciable gain in $C_{L,max}$ because leading-edge stall occurred at an angle of attack of approximately 8°. Drooping the leading edge 40° produced a maximum lift coefficient of 1.35 at an angle of attack of 14°. Tuft studies

made in conjunction with these force tests showed that for the higher droop angles the $C_{L,max}$ was limited by stall occurring first on the outboard wing section and originating behind the knee of the nose droop. If lower droop angles were used, separation at the leading edge became predominant and higher lift coefficients could not be reached without some supplementary flow control.

Effect of blowing with nose droop.- The results of tests with the nose drooped and blowing being applied either from a slot at the wing leading edge (nose slot) or from a slot at the contour change caused by the droop (knee slot) are presented in figures 8 to 14. It was found that blowing applied at the leading edge (when applied from a full-span slot or a partial-span slot) increased both maximum lift coefficient and angle of attack for maximum lift for several variations in spanwise distribution of blowing-momentum coefficient (figs. 8 and 10). For the partial-span blowing conditions, tuft observations (figs. 9 and 11) showed some slight flow roughness emanating behind the knee of the droop on the inboard wing stations. This roughness, even though not severe, seemed to have a detrimental effect on lift. However, when blowing at the leading edge was applied to this area of the wing, only a very small amount of air was required to eliminate the separation, and the resulting maximum lift coefficients $\left(C_{L,max} = 1.65\right)$ were about equal at $\alpha = 19^{\circ}$ for either blowing condition (fig. 10).

Perhaps it should be pointed out here that inboard leading-edge separation was not severe on this configuration because drooping the nose gave fairly large radius-contour changes which were not critical for early stall precipitation. On thinner wings, a drooped-nose configuration would have less-favorable geometric characteristics, that is, the sharper contour changes would be conducive to early flow separation at the leading edge and would, therefore, require blowing at the leading edge from a full-span slot. The results of tests made in an attempt to determine minimum leading-edge C_{μ} requirements (figs. 8 and 10) show that, although the inboard requirements were very small, the values of momentum coefficient at the wing-tip section could not be lowered appreciably below 0.01 without lift losses due to tip stall. With total leading-edge momentum coefficient as low as 0.014, nearly linear lift curves were obtained to maximum lift coefficients of approximately 1.6 at an angle of attack of 19°. This leading-edge flow rate, added to the minimum boundary-layer control-flap condition $\left(C_{\mu,f} = 0.010\right)$, would give total airplane requirements within the limits allowed for current compressor bleed systems.

Limited tests were made of blowing at the nose slot with the nose undeflected, and the results failed to show any lift gains because of the inability to control flow separation at the leading edge by blowing alone. Observation of nose pressures on a manometer showed that the nose

slot in the center and outboard compartments was not sufficiently forward to have any effect on separation caused by the large adverse pressure gradient at the nose. However, tests showed that, once the leading edge was drooped, the air ejected from the nose slot negotiated the curvature at the knee of the droop and remained attached to the wing surface some distance behind the knee. It is thought that this is the reason why the results of nose and knee blowing were as comparable as they were for the drooped-nose configuration. The knee slot, therefore, from a design and maintenance viewpoint, may be a more practical arrangement on an airplane wing having thin sections with very small nose radii.

In order to determine the effects of increased flap blowing-momentum coefficient on the leading-edge blowing requirements, flap blowing-momentum coefficients were increased tenfold to values of 0.10 and 0.18. The variations of nose and knee spanwise-compartment momentum coefficients (figs. 12 and 13) indicate essentially the same wing flow characteristics as were evidenced with the lower flap blowing rate ($C_{\mu,f} \approx 0.03$). Blowing applied at the leading edge in about the same proportion and spanwise distribution as for the lower flap blowing rates was effective in producing relatively clean flow over the wing span to high angles of attack ($\alpha = 18^\circ$). With the higher flap blowing conditions ($C_{\mu,f} = 0.10$ and 0.18), flow on the flap was not as sensitive to disturbances emanating from the wing root. In this respect, blowing over the leading edge of the partial span (outboard $0.534b/2$) did not have the slightly adverse effect on lift as was noted by the roughness at the inboard end of the slot for the lower flap blowing rates. With flap blowing-momentum coefficients of the order of 0.18, however, the sections outboard of the end of the flap experienced much higher induced upwash and caused flow separation at the leading edge on that area of the wing. Consequently, it was necessary to increase the flow rates of the outboard slot in order to maintain unseparated flow behind the knee (fig. 13). For the flap condition $C_{\mu,f} = 0.10$ (fig. 12), partial- and full-span blowing from either the nose or knee slots of the drooped leading edge gave about the same maximum lift and angle of attack ($C_{L,max} = 1.8$ and $\alpha = 18^\circ$, respectively). Also, for the higher flap momentum coefficients, the lift-curve slope was maintained more nearly linear to higher angles of attack.

In order to determine the effectiveness of blowing at the knee of a drooped leading edge when applied to a thin swept wing having zero leading-edge radius, the model was fitted with a sharp leading edge (see fig. 3). Several tests were made at flap momentum coefficients of 0.03 and 0.10 for the drooped-nose configuration with and without knee blowing, and these results (fig. 14) were comparable to those for the normal nose. Tuft observations during the test proved interesting in that a very tightly bound vortex remained attached to the leading edge up to angles of attack near maximum lift. This leading-edge vortex did not induce

separation behind the drooped nose (as might have been expected at lower angles of attack than for the round nose); and as a result, the blowing requirements for controlling the separation behind the knee was about the same for either the sharp- or rounded-leading-edge configuration. However, a sharp-leading-edge droop would be expected to introduce more influence on the phenomenon of flow separation at the tip and requirements for blowing at the leading edge for wings of less leading-edge sweep.

Effect of leading-edge-radius increase.- The limited wind-tunnel tests (ref. 1) of a nose radius- and camber-increase configuration showed this modification (fig. 3) to have good leading-edge stall-control capabilities at somewhat higher angles of attack with the application of partial-span leading-edge-blowing boundary-layer control. It was, therefore, of interest to investigate the radius increase over a wider range of leading-edge blowing-momentum coefficients and with blowing over the leading edge from a full-span slot.

Wind-tunnel tests were conducted to determine the stall-control effectiveness of the nose radius and camber increase for model configurations as follows: flap neutral, flap deflected with no boundary-layer control, flap deflected with flap boundary-layer control, and flap deflected with blowing over both the wing leading edge and flap. These data are presented in figures 15 to 20.

The radius increase had no effect on the model characteristics over the lower lift range (fig. 15), but adding the increased radius did extend the linear part of the lift curve to a higher angle of attack (to about 13°) than was noted for the basic nose. The added radius and camber alone were not sufficient leading-edge treatment to delay flow separation at the leading edge above an angle of attack of about 13°. Similar results were also noted for tests with blowing applied to the trailing-edge flap (fig. 16) for a range of flap momentum coefficient from 0 to 0.180.

Effect of blowing with increased nose radius.- The results of blowing over the increased nose radius show a marked effect for variation in spanwise blowing application. These findings are graphically shown in the lift curves of figure 17 in which blowing is applied in successive tests to the outboard 0.33b/2, outboard 0.53b/2, and 0.85b/2 nose slots, respectively. It is seen that, as the spanwise extent of blowing was increased, large gains in lift were obtained; whereas, increasing blowing rates for partial span blowing gave only small improvements for comparable total C_{μ} values. It will be noted also in figure 17 that, as the spanwise application of boundary-layer control is extended from the tip toward the wing root, the lift curves, at high angles of attack, become more linear as the maximum lift coefficient is increased. This is due to the elimination of the flow separation at the leading edge and subsequent losses of lift on the inboard wing sections. The nose

with a radius increase, having less camber effect than the drooped nose at these wing stations, was not capable of controlling the stall at the leading edge induced by blowing on the flap. Tuft observations (fig. 18) made in conjunction with the force tests showed flow separation at the leading edge on this region of the wing at an angle of attack of about 12°. At the lower flap blowing rates, this disturbance on the wing inboard also had a detrimental effect on flap effectiveness at the higher angle of attack. Blowing at the leading edge, in eliminating this localized flow separation at the nose, not only restored wing lift but also allowed the flap to maintain full effectiveness to higher angles of attack. Consequently, with good lift capabilities maintained on all stations of the wing to fairly high angle of attack, the lift curves are substantially linear to maximum lift ($C_{L,max} = 1.8$) where a sharp break is noted as the wing stalls at $\alpha = 22°$.

For slightly higher flap blowing rates ($C_{\mu,f} = 0.025$ in fig. 19), blowing over the leading edge from a half-span slot at a substantial total leading-edge value of momentum coefficient ($C_{\mu,LE} = 0.025$) was again not as effective as using approximately the same amount of air redistributed in a full-span application. Since the attainment of the high lift coefficient at the high angle of attack is restricted by the landing geometry of the airplane design in many cases, it may be noted in figure 19 that the undesirable sudden-stall characteristic can be alleviated by reducing the blowing over the inboard wing stations.

It was of interest to know whether leading-edge boundary-layer control would be effective when applied in combination with a trailing-edge system using a large percentage of engine thrust to augment lift. A few tests were, therefore, made with very high flap momentum coefficients covering a range from 0.100 to 0.369. These results (fig. 20) show that a linear lift curve could be maintained to a rather high lift coefficient ($C_L = 2.33$); but as indicated before for the drooped nose, it was necessary to increase the blowing rate over the outboard nose sections in order to prevent the wing tip from stalling.

Pitching-Moment Characteristics

The pitch-up characteristics of sweptback wings have long been one of the leading stability problems caused by the forward shift of the center of pressure as the wing tips stalled. It was hoped that the present investigation would show that, with the proper distribution of blowing at the leading edge, the pitch-up at $C_{L,max}$ might be eliminated. However, even for the tests with blowing over only the outboard $0.54b/2$ of the wing leading edge, some tendency toward pitch-up still persisted, regardless of the amount of blowing applied.

Both the configuration for the drooped nose and for the leading-edge-nose radius increase, in general, exhibited similar longitudinal stability characteristics. The pitching-moment data show the model to be longitudinally stable up to the maximum lift coefficients with a tendency to pitch up at stall. The application of boundary-layer control to the flap or leading edge had no appreciable effect on the magnitude of the pitching moments in the normal lift range, and the moment curves remained linear with almost constant slope up to $C_{L,max}$.

The horizontal tail on this model was mounted with zero incidence on the wing chord plane extended. For the flap configuration without boundary-layer control, with a partial-span leading-edge device which was adequate to prevent tip stall, the tail was in a favorable downwash gradient and thus produced stability through the stall. The failure to produce a stable pitching-moment break for any of the flap boundary-layer-control configurations is considered to be associated with the increased downwash inboard behind the highly loaded wing which creates a less favorable downwash field for the tail and prevents the tail contribution from overcoming the unstable moments of the wing. On the basis of some preliminary downwash measurements obtained during this investigation, it is believed that a slightly lower tail position ($0.11\bar{c}$ below the wing chord line) would result in a less-unstable configuration of $C_{L,max}$.

It should be noted that, for the very high flap C_μ conditions ($\gtrapprox 0.100$), the pitching moments would be beyond the trim capabilities of a normal tail configuration even for a conventional static margin. For the more moderate flap C_μ conditions ($\lessapprox 0.03$), however, the all-movable tail as tested would be fully capable of trim for center-of-gravity positions representing realistic static margins. For example, with a center-of-gravity position of 37 percent mean aerodynamic chord which gives a static margin of 0.12 for the landing configuration, trim-lift coefficients of the order of 1.45 to 1.5 could be attained for blowing conditions compatible with a compressor bleed air supply, with mass-flow rates ranging upward to 10 pounds per second.

Many airplanes without boundary-layer control employing the current leading-edge stall control and trailing-edge high-lift devices are limited to maximum landing attitude angles of about 12° because of the contact of the tail with the ground. In figure 7 it is noted that an angle of 12° is very near maximum lift for the configuration without blowing at the leading edge. For these same ground-contact attitudes, a boundary-layer-control airplane using an arrangement such as the one employed in this investigation (droop 40°, flaps 60°) not only shows a higher lift coefficient at equivalent angles but also has the lift curve extended to angles of attack (some 8° higher) considerably beyond the contact attitude. With this in mind, then, it might be well to note that, since the pitching-moment curves are practically linear to maximum lift, the

margin of C_L and α between touchdown attitude and stall angle may be looked upon as the region above the $0.85C_{L,max}$ condition usually considered for safe landing.

Drag Characteristics

In general, the drag data (figs. 4 to 20) of this investigation are characteristic of the results of other boundary-layer-control applications on wind-tunnel and flight-test models (refs. 1 to 4). It is noted that the high lift configurations with the boundary-layer control displayed higher drag coefficients in the lower C_L range than with no boundary-layer control. (See fig. 7.) These increases in drag are generally attributed to the change in induced drags. Although the elimination of separation on the flap by boundary-layer control would tend to reduce the profile drag of the configuration, an appreciable increase in induced drag would be anticipated for the wing span loading resulting from the increased lift coefficients on the inboard wing sections affected by boundary-layer control on the flap. It has been shown in reference 1 that high lifts can be obtained with lower drag coefficients for a boundary-layer control system with full-span flap because of the more uniform span loading. However, on the highly swept wing, the large pitching moments, resulting from the full-span configuration, produced trim requirements that negate the use of the lift gained from the full-span flap.

For comparison purposes, the partial-span leading-edge slat configuration with flaps deflected 40° (ref. 1) was chosen to represent a typical fighter airplane having no boundary-layer control. Lift-drag ratios for this configuration and those of the present boundary-layer-control configuration (flaps 60°, droop 40°; see fig. 8) are presented in figure 21. The customary increase with C_L is noted for L/D of the configuration without boundary-layer control, with maximum values of L/D of about 5.6 occurring at $C_L \approx 0.9$, and then L/D decreases rapidly with further increase in C_L which indicates a rapid drag increase as flow separation sets in on the wing. When compared with a boundary-layer-control high-lift configuration such as the one previously mentioned, it is noted that, with wing and flap separation controlled by boundary-layer control, the lift-drag ratio, although not as high, presents a much flatter curve in the high lift range and is extended to a somewhat higher lift coefficient ($C_L = 1.25$).

In order to point out, perhaps more graphically, the effects of boundary-layer control on the handling characteristics and the speed reduction possible during the landing phase of a typical fighter airplane, figure 22 was prepared. This airplane was assumed to have a

wing area of 325 square feet and a wing loading of 60 pounds per square foot. For the boundary-layer-control condition, the data of figure 8 were adjusted to trim-lift coefficients for a static margin dC_m/dC_L of 12 percent. The thrust required was determined by the equation $T = C_D qS$. Since these test data were for a constant stabilizer setting and constant blowing-momentum coefficient, the C_D values were adjusted to account for the increment of drag due to tail deflection required for trim and for the variation in the momentum coefficient assuming constant-bleed air flow for flight velocities from 110 to 190 knots.

It is noted in figure 22 that the thrust required decreases with velocity to a point corresponding to the angle of attack for best L/D and then begins to rise sharply. The portion of the curve indicating sharp increase in thrust required is the region in which the pilot usually experiences difficulty in establishing steady-flight conditions and is generally known as the back side of the power curve. Consequently, landing-approach speeds are higher than values for minimum thrust. For the configuration without boundary-layer control, this condition occurred at a velocity of about 130 knots; but for the configuration with boundary-layer control applied, it can be seen that the speed may be reduced about 15 knots below that value before the drag rise occurs. Another item of importance is that, although the level of thrust required is higher throughout the speed range for the boundary-layer-control configuration, the rate of increase of thrust with reduced velocity approaching $C_{L,max}$ is not as great as indicated for the case without boundary-layer control. In addition to improved low-speed handling characteristics, pilots report (ref. 3) that the reduced attitude improves visibility considerably for landing. It is seen that, as speed reductions occur for both models, the boundary-layer-control model has attitudes considerably below those of the model without boundary-layer control at a given velocity, and that the greatest difference is at minimum thrust for the model without boundary-layer control.

In order that the aforementioned conditions may be obtained, the assumption must be made, of course, that the overall low-speed characteristics of the airplane are acceptable to the pilot.

CONCLUSIONS

An investigation in the Langley full-scale tunnel on the effect of high-pressure blowing at the leading edge as a means of boundary-layer control on the aerodynamic characteristics of a 49° swept-wing complete model has resulted in the following conclusions:

1. Neither leading-edge droop nor leading-edge-radius increase used as a leading-edge control device proved adequate to control flow separation at the leading edge when accompanying an effective flap boundary-layer-control configuration.

2. Blowing at the wing leading edge with only moderate values of momentum coefficient used in combination with droop or increased leading-edge radius increased the effectiveness of both devices and, consequently, extended the angle-of-attack range and maximum lift coefficient appreciably.

3. Because of the mechanical difficulty of constructing a nose slot sufficiently forward on thin wings to control flow separation at the leading edge, blowing at the nose alone was ineffective for the basic airfoil section. The addition of droop or radius increase was required in order to achieve effective stall control.

4. For the drooped-nose configuration, blowing from either the slot at the knee of the droop or the slot located on the upper surface near the leading edge produced similar gains in lift.

5. Blowing at the leading edge of the wing for either nose droop or radius increase produced little change in pitching moment at a given lift coefficient below the maximum lift coefficient. The pitching-moment curves were substantially linear up to the maximum lift coefficient with a slight pitch-up characteristic at stall.

6. A properly designed boundary-layer-control high-pressure blowing system requiring a total mass-flow rate within the bleedoff capabilities of current turbojet compressors could be expected to reduce the approach speed by about 15 knots when applied to a typical airplane configuration having a wing loading of 60 pounds per square foot. This assumes that in all other respects the handling qualities and stall-warning characteristics are found satisfactory at the higher operating lift coefficients.

Langley Aeronautical Laboratory,
National Advisory Committee for Aeronautics,
Langley Field, Va., April 4, 1957.

REFERENCES

1. McLemore, H. Clyde, and Fink, Marvin P.: Blowing Over the Flaps and Wing Leading Edge of a Thin 49° Swept Wing-Body-Tail Configuration in Combination With Leading-Edge Devices. NACA RM L56E16, 1956.

2. Koening, David G., and Aoyagi, Kiyoshi: Large-Scale Wind-Tunnel Tests of an Airplane With a 45° Sweptback Wing of Aspect Ratio 2.8 With Area Suction Applied to Trailing-Edge Flaps and With Several Wing Leading-Edge Modifications. NACA RM A56H08, 1956.

3. Anderson, Seth B., Quigley, Hervey C., and Innis, Robert C.: Flight Measurements of the Low-Speed Characteristics of a 35° Swept-Wing Airplane With Blowing-Type Boundary-Layer Control on the Trailing-Edge Flaps. NACA RM A56G30, 1956.

4. Kelly, Mark W., and Tolhurst, William H., Jr.: Full-Scale Wind-Tunnel Tests of a 35° Sweptback Wing Airplane With High-Velocity Blowing Over the Trailing-Edge Flaps. NACA RM A55I09, 1955.

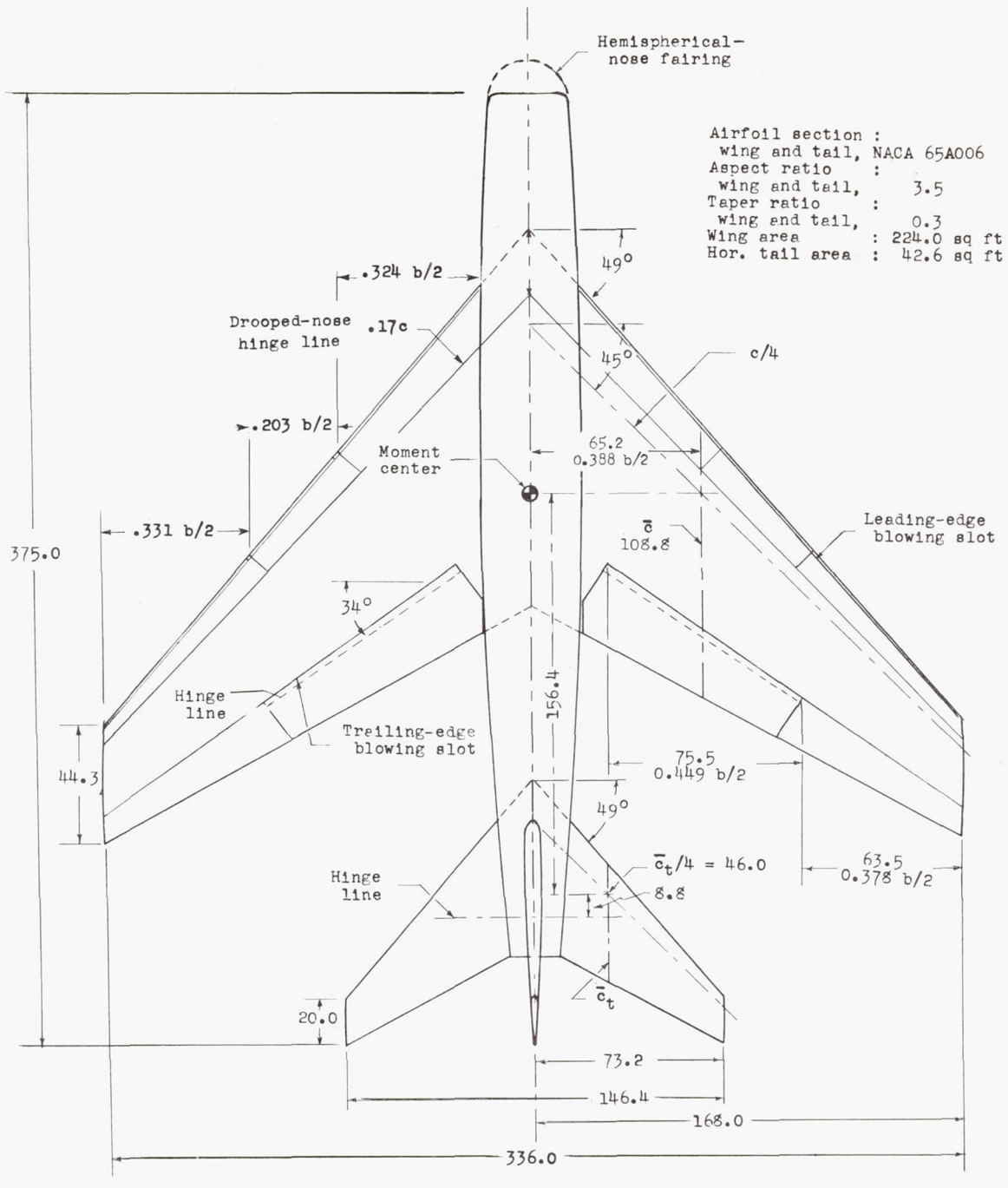

Figure 1.- Geometric characteristics of the model. All dimensions are in inches.

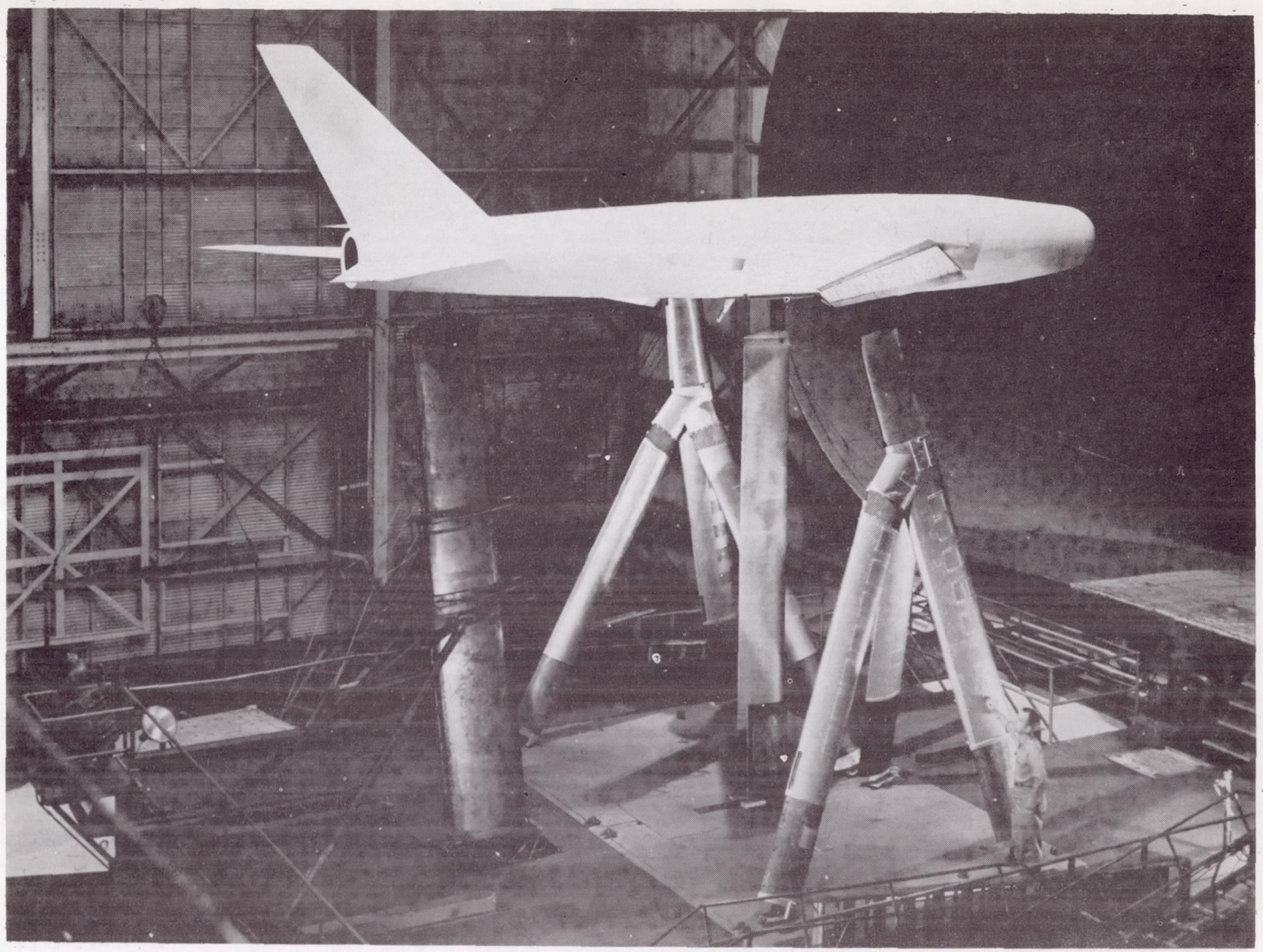

Figure 2.- General view of model mounted in wind tunnel. L-93853

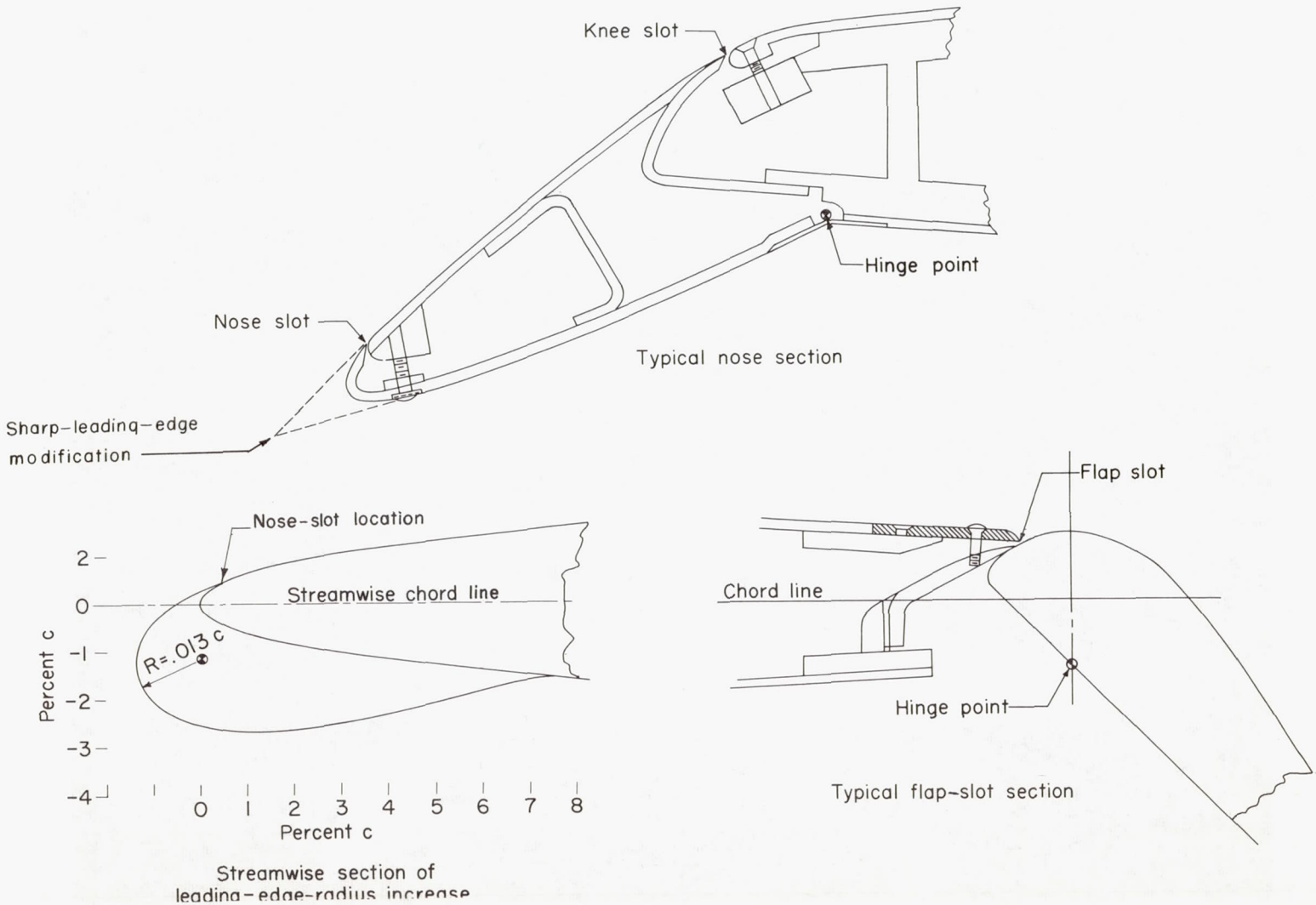

Figure 3.- Typical cross-sectional views of leading-edge drooped nose, nose with radius increase, and trailing-edge-flap blowing slot.

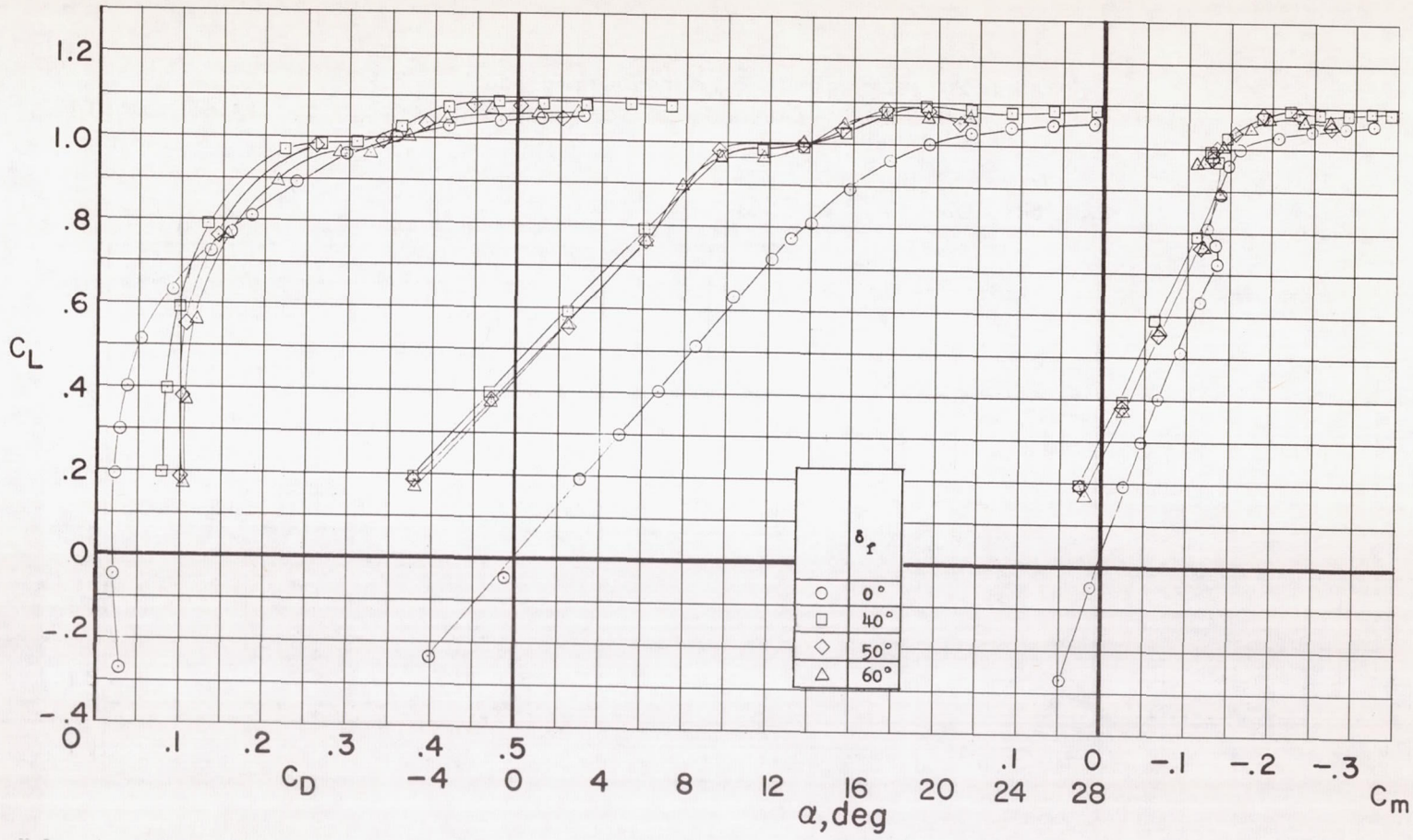

Figure 4.- Model characteristics with trailing-edge flaps deflected. Basic leading edge.

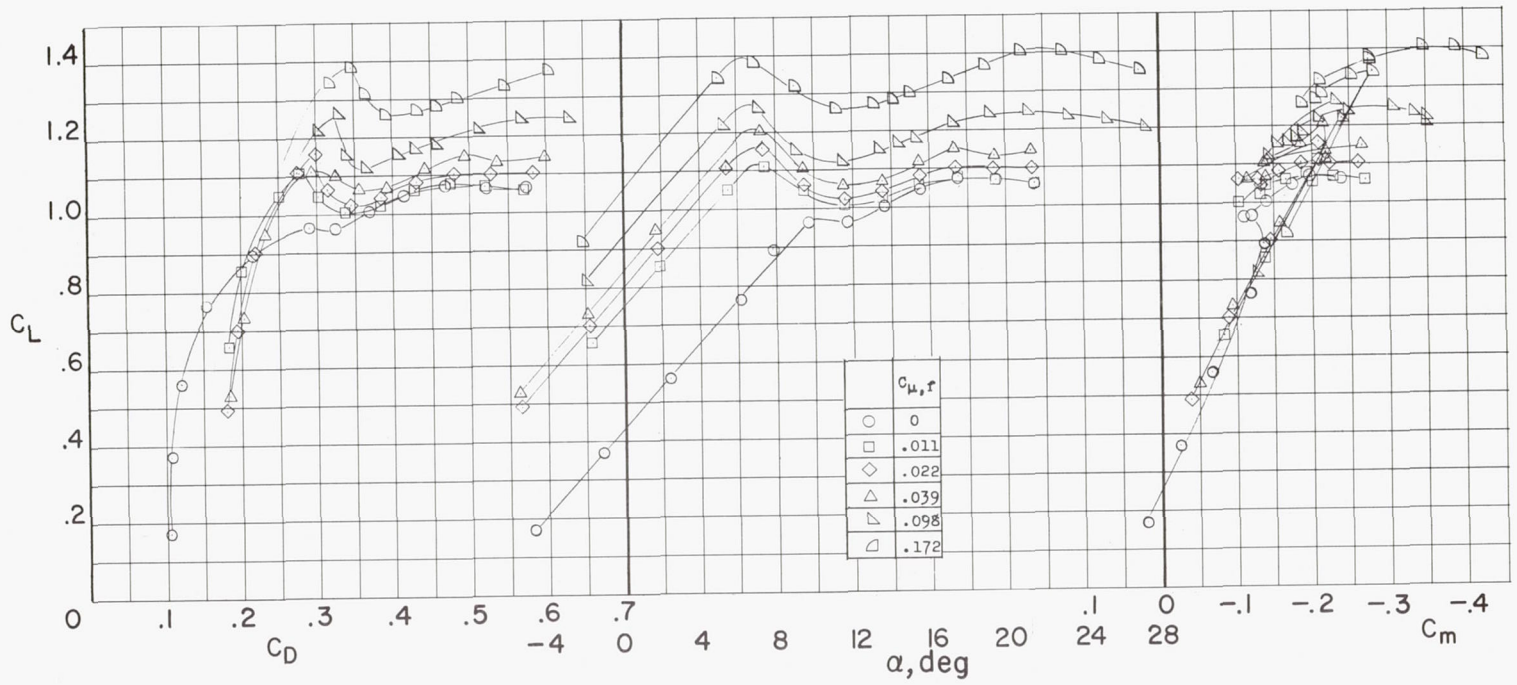

Figure 5.- Effect of flap-blowing type of boundary-layer control on model with trailing-edge flaps deflected 60°. Basic leading edge.

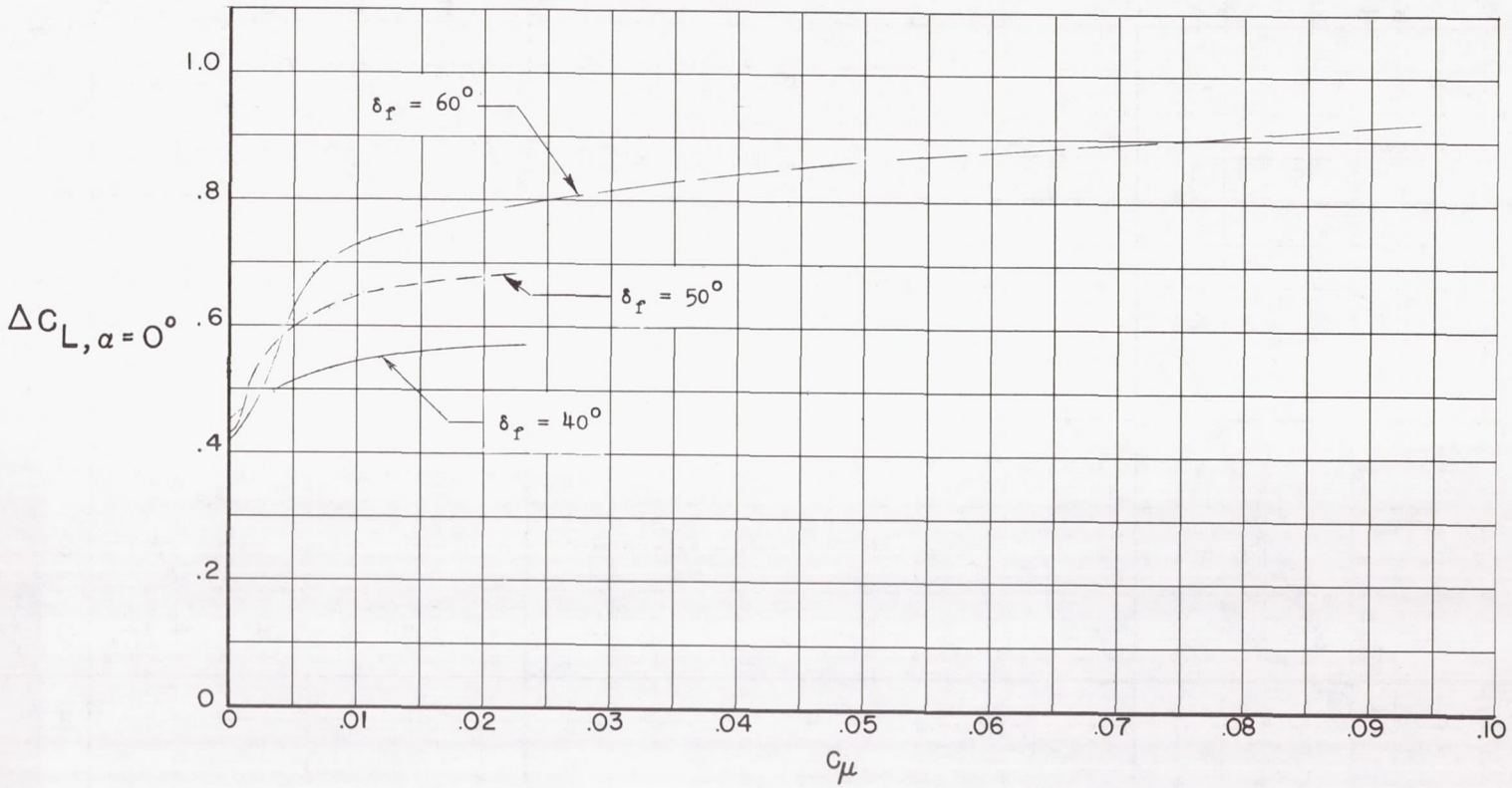

Figure 6.- Variation of incremental lift coefficient with momentum coefficient.

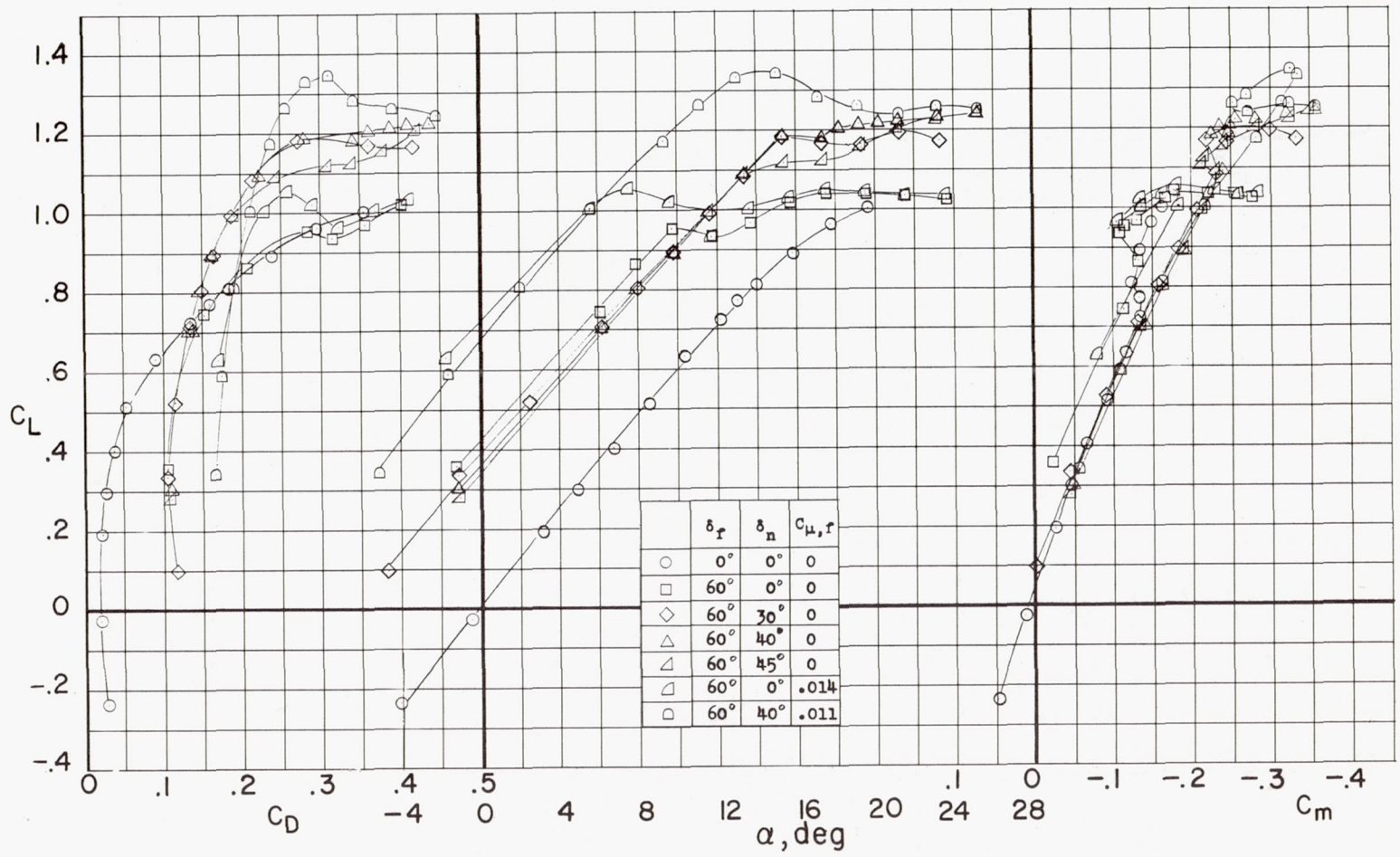

Figure 7.- Effect of nose droop in conjunction with trailing-edge-flap deflection without and with blowing over the flap. $\delta_f = 60^\circ$.

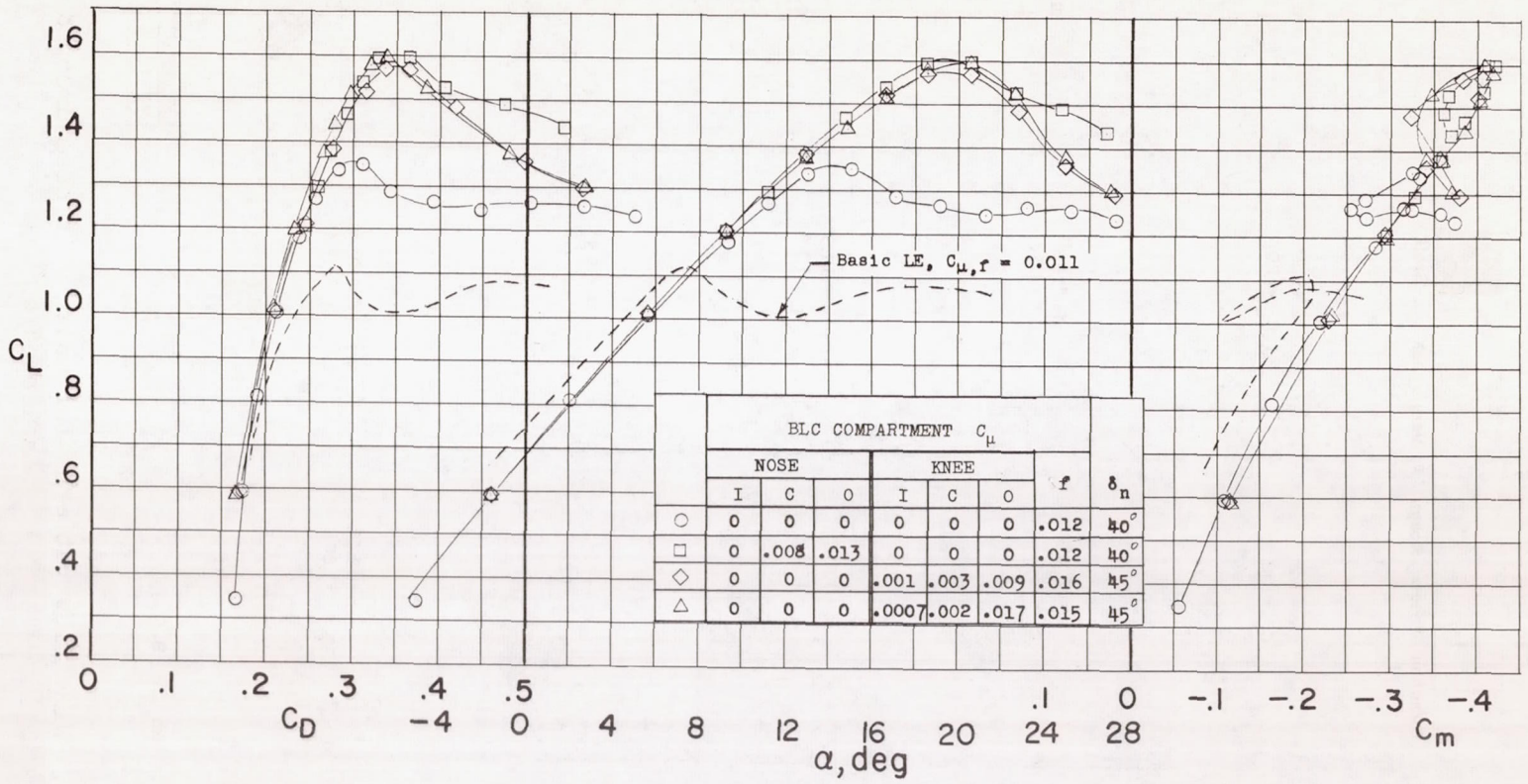

Figure 8.- Effect of nose droop in conjunction with blowing over the leading edge and flap. $\delta_f = 60^\circ$.

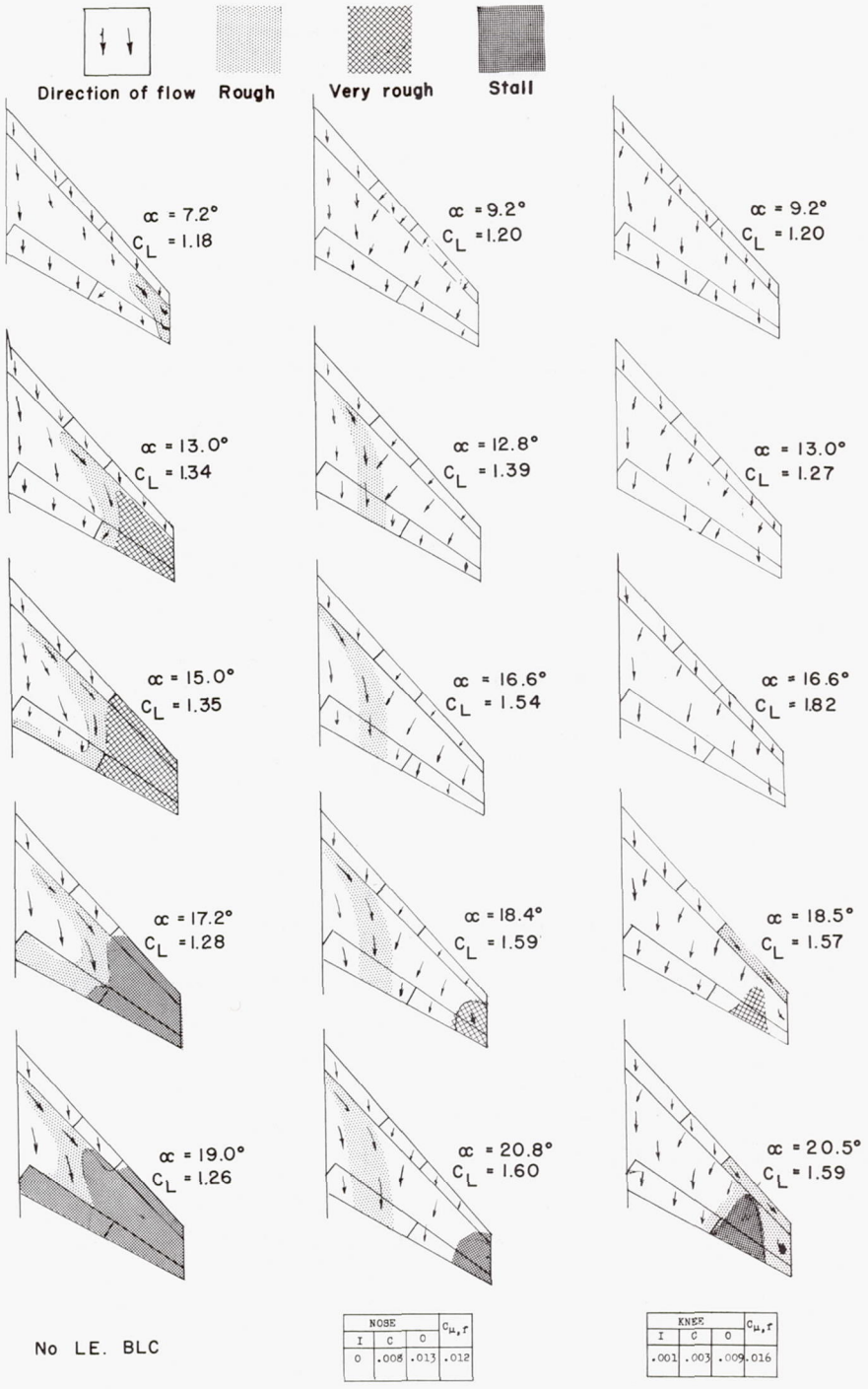

Figure 9.- Wing flow patterns for model with nose drooped 40° and flaps deflected 60°.

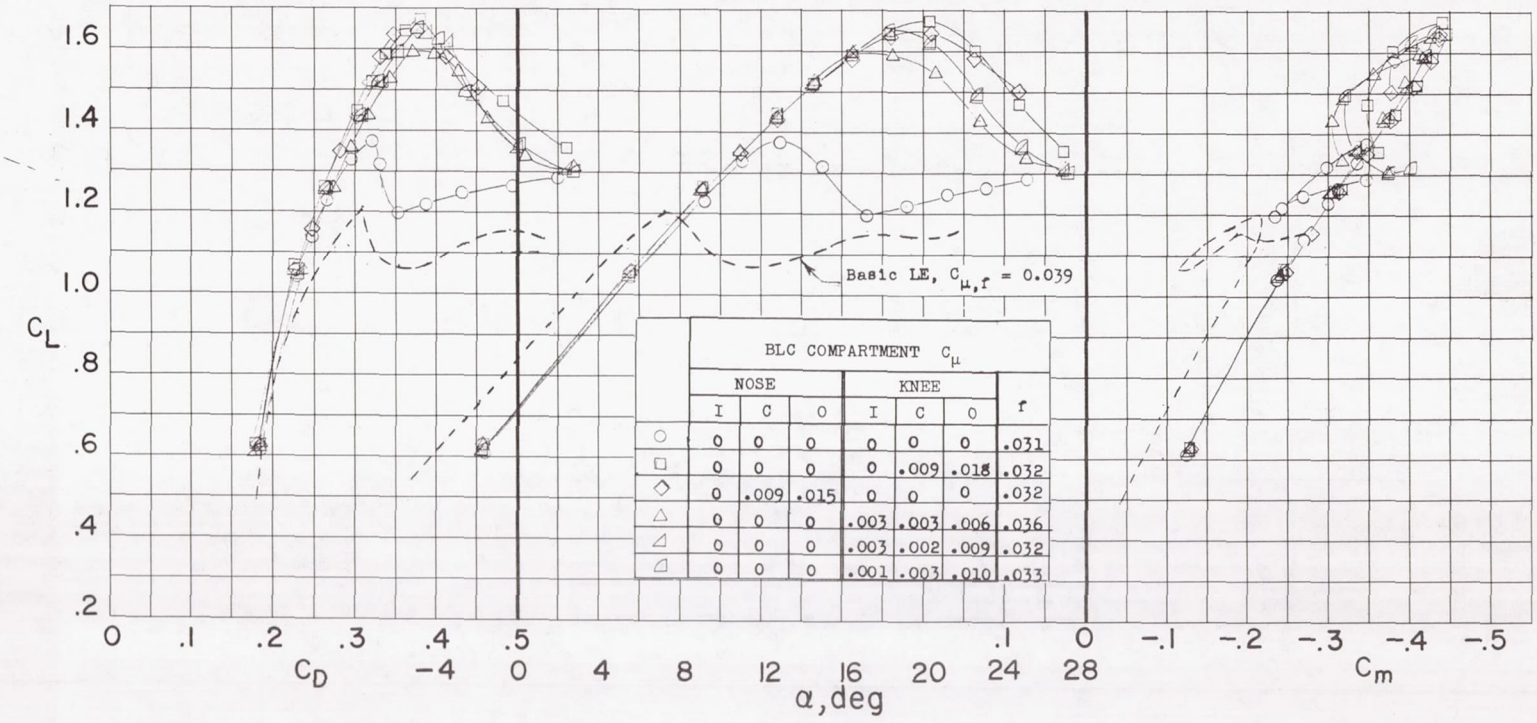

Figure 10.- Effect of nose droop in conjunction with blowing over the leading edge and flap. $\delta_f = 60°$.

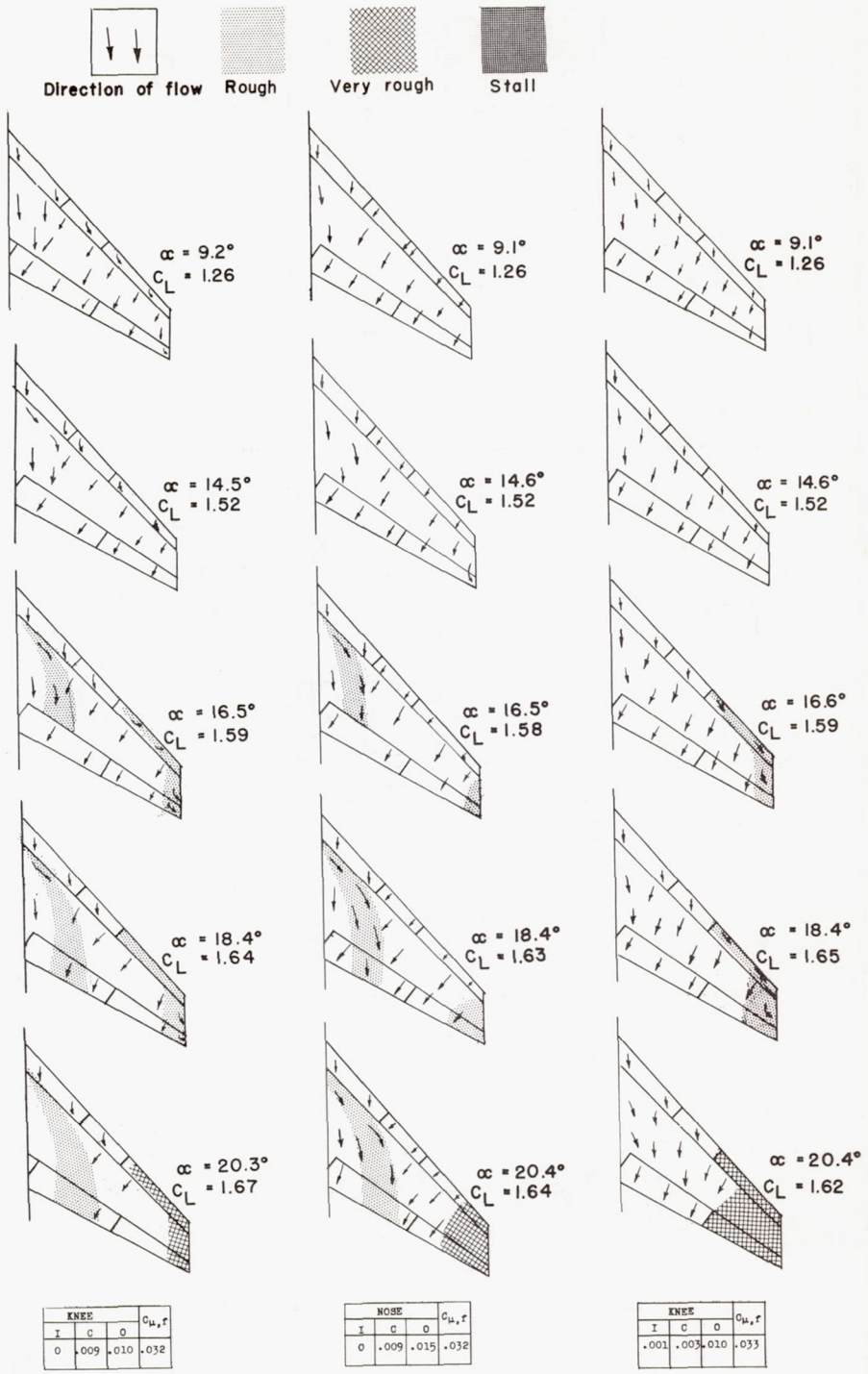

Figure 11.- Wing flow patterns for model with nose drooped 40° and flaps deflected 60°.

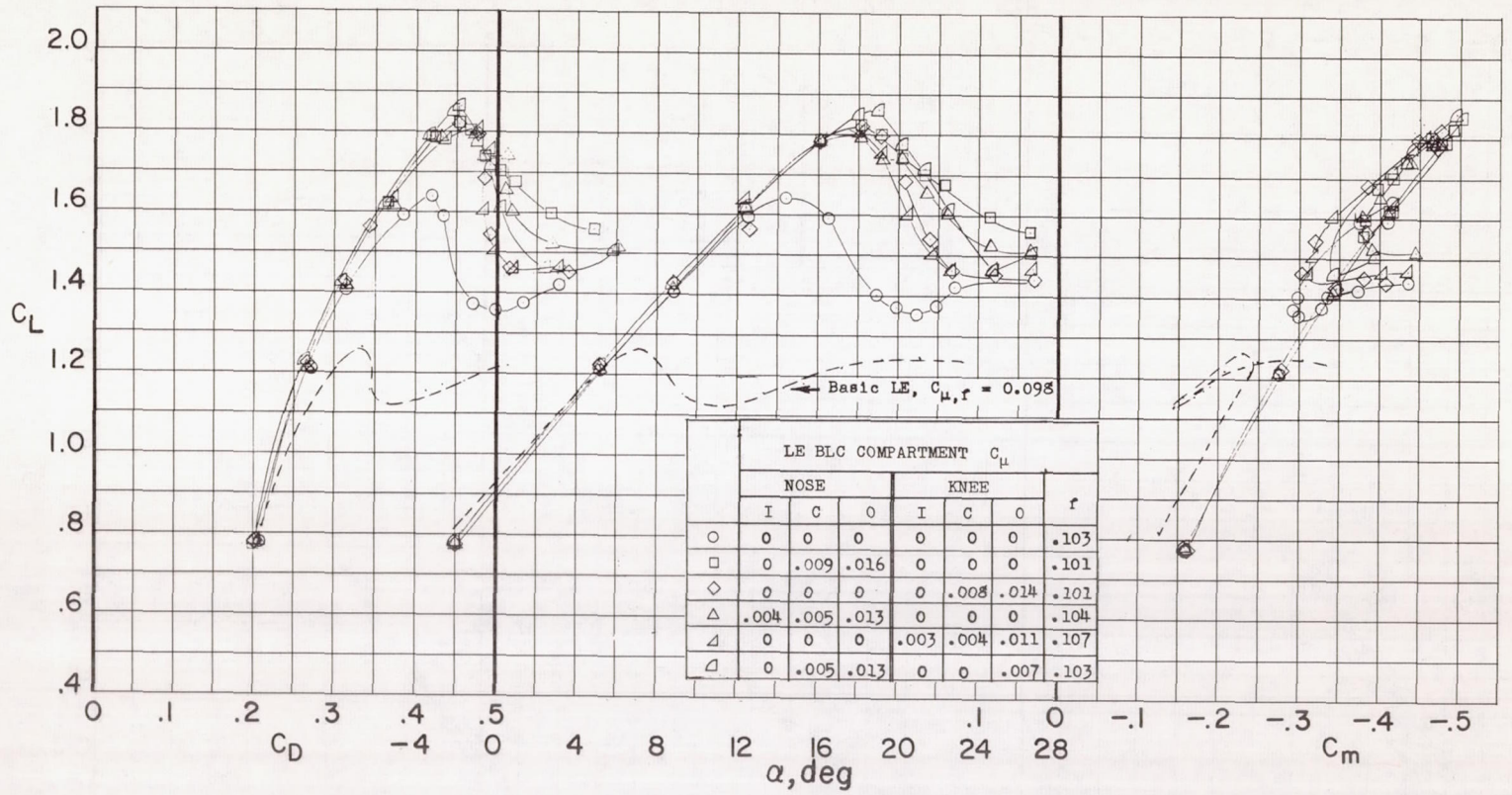

Figure 12.- Effect of nose droop in conjunction with blowing over the leading edge and flap. $\delta_f = 60^\circ$.

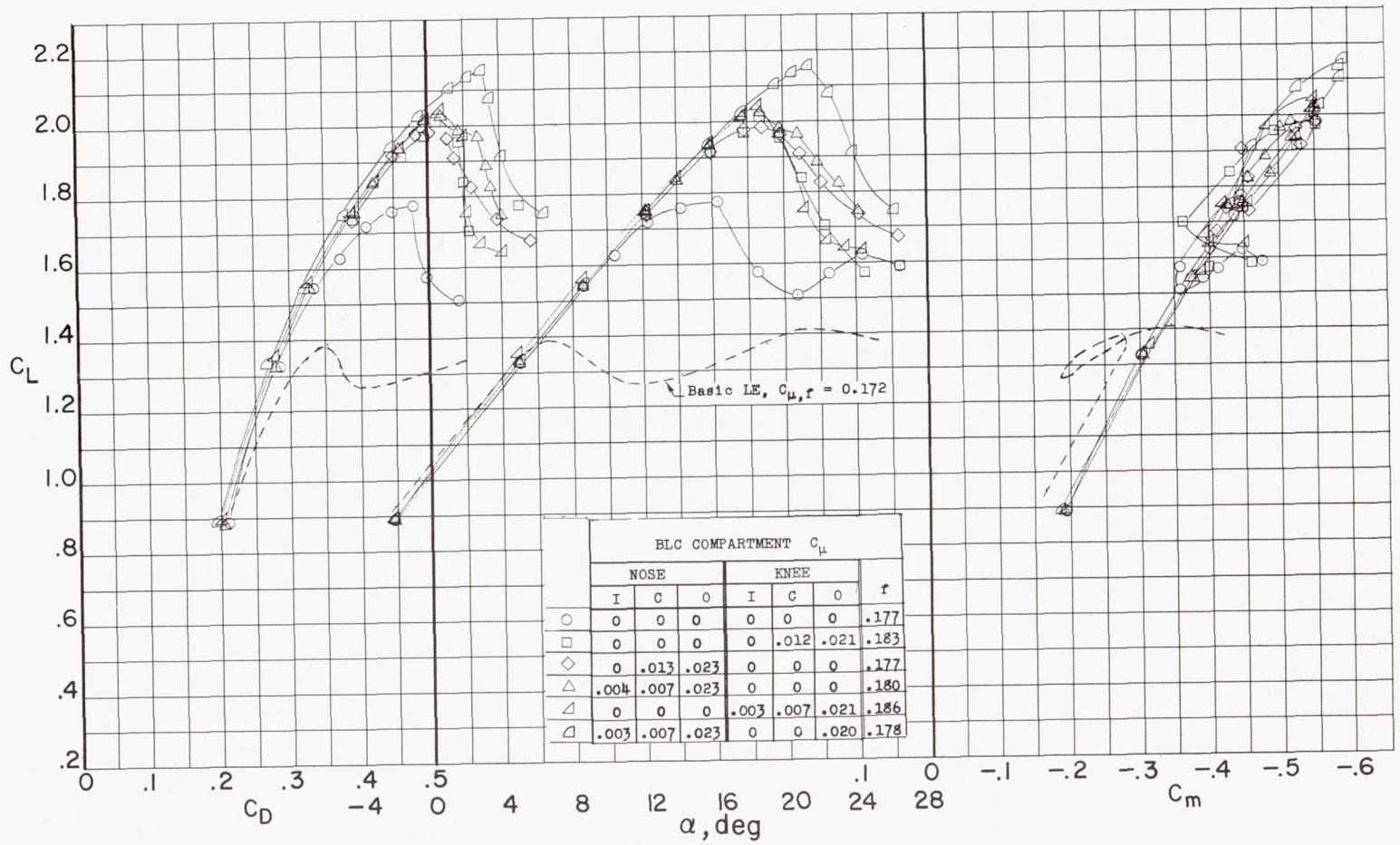

Figure 13.- Effect of nose droop in conjunction with blowing over the leading edge and flap. $\delta_f = 60^\circ$.

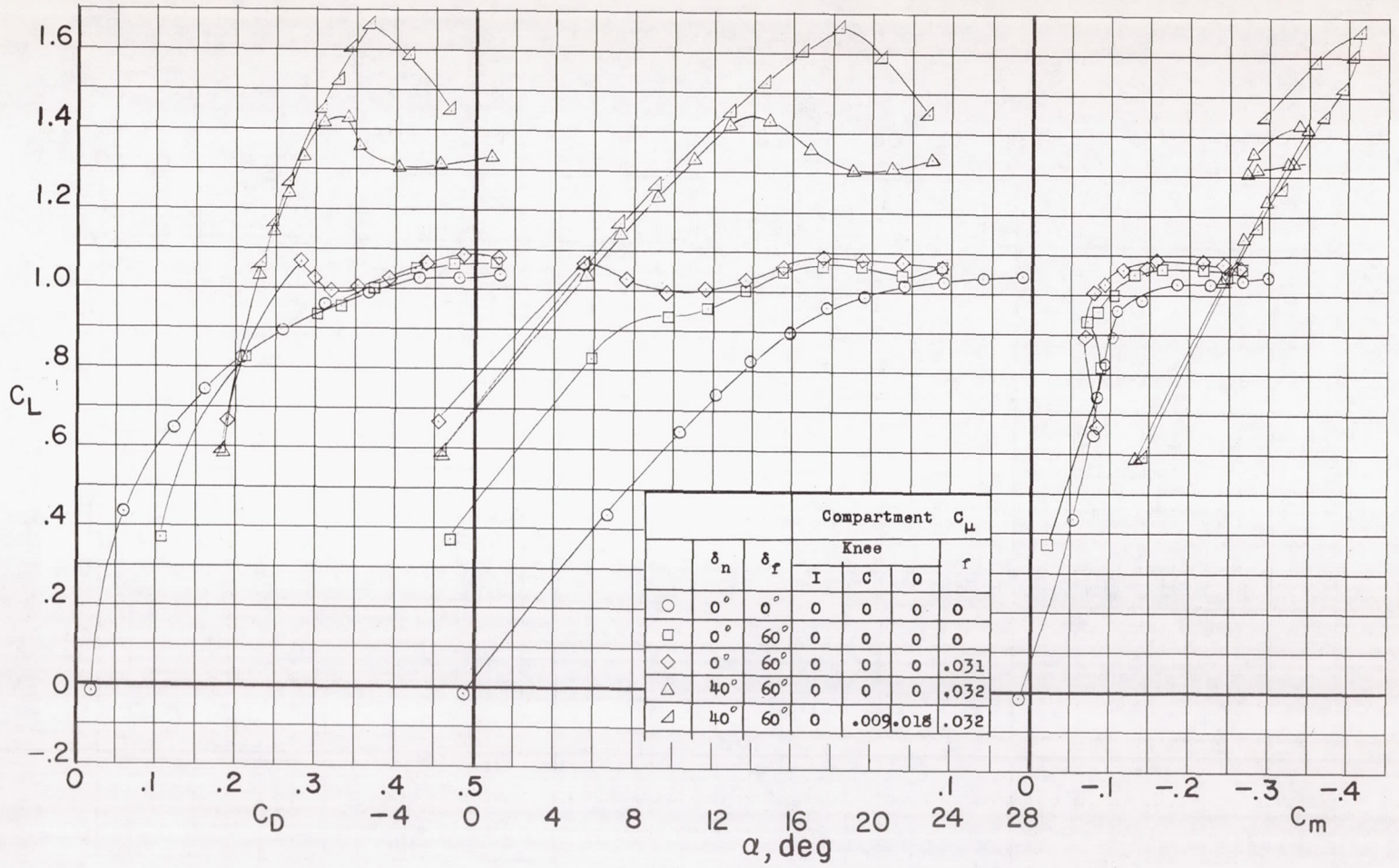

Figure 14.- Model characteristics for the sharp-nose modification for configurations as follows: basic model, flap deflection, with and without flap blowing, and nose droop with and without blowing at the leading edge.

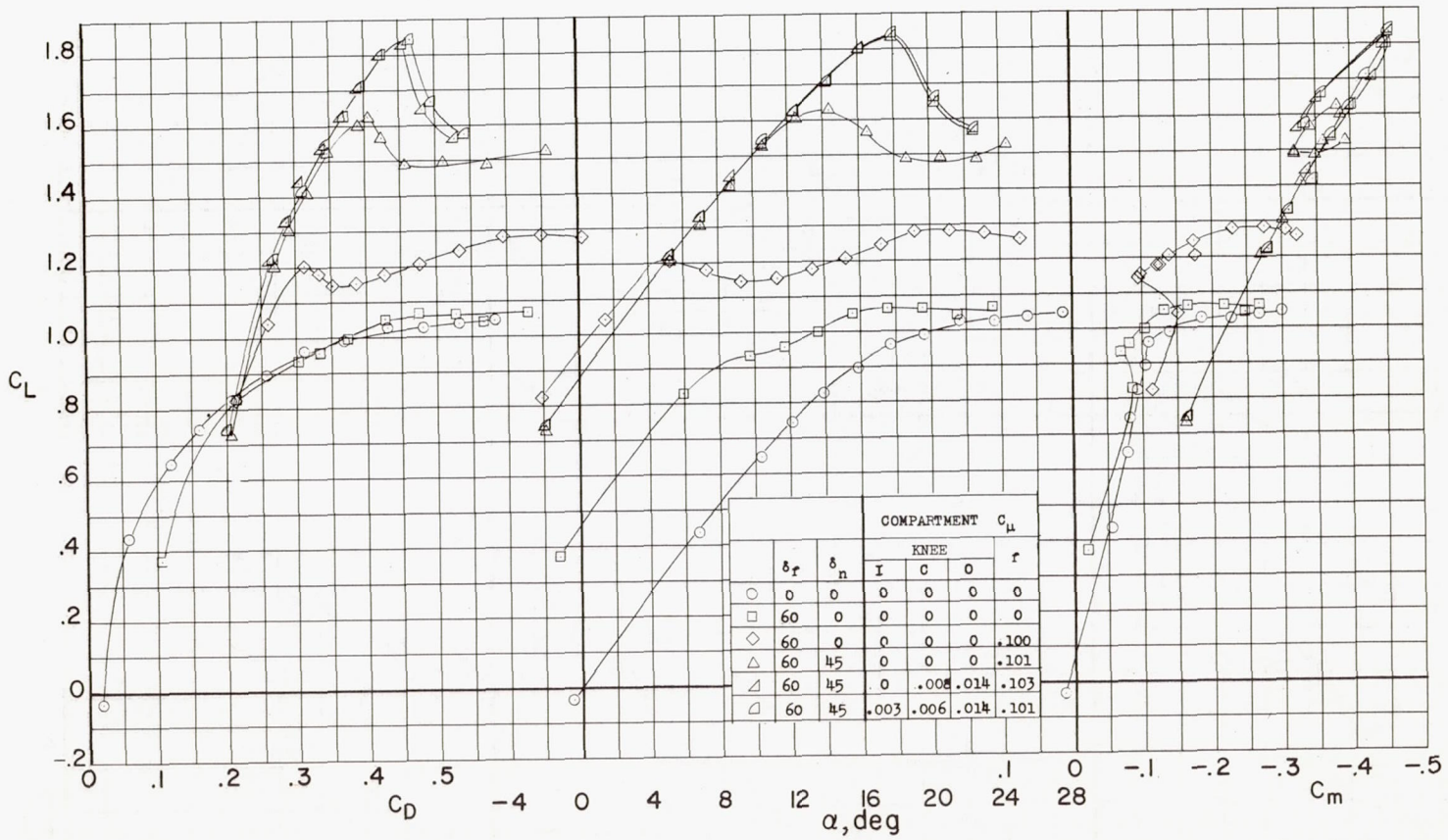

Figure 14.- Concluded.

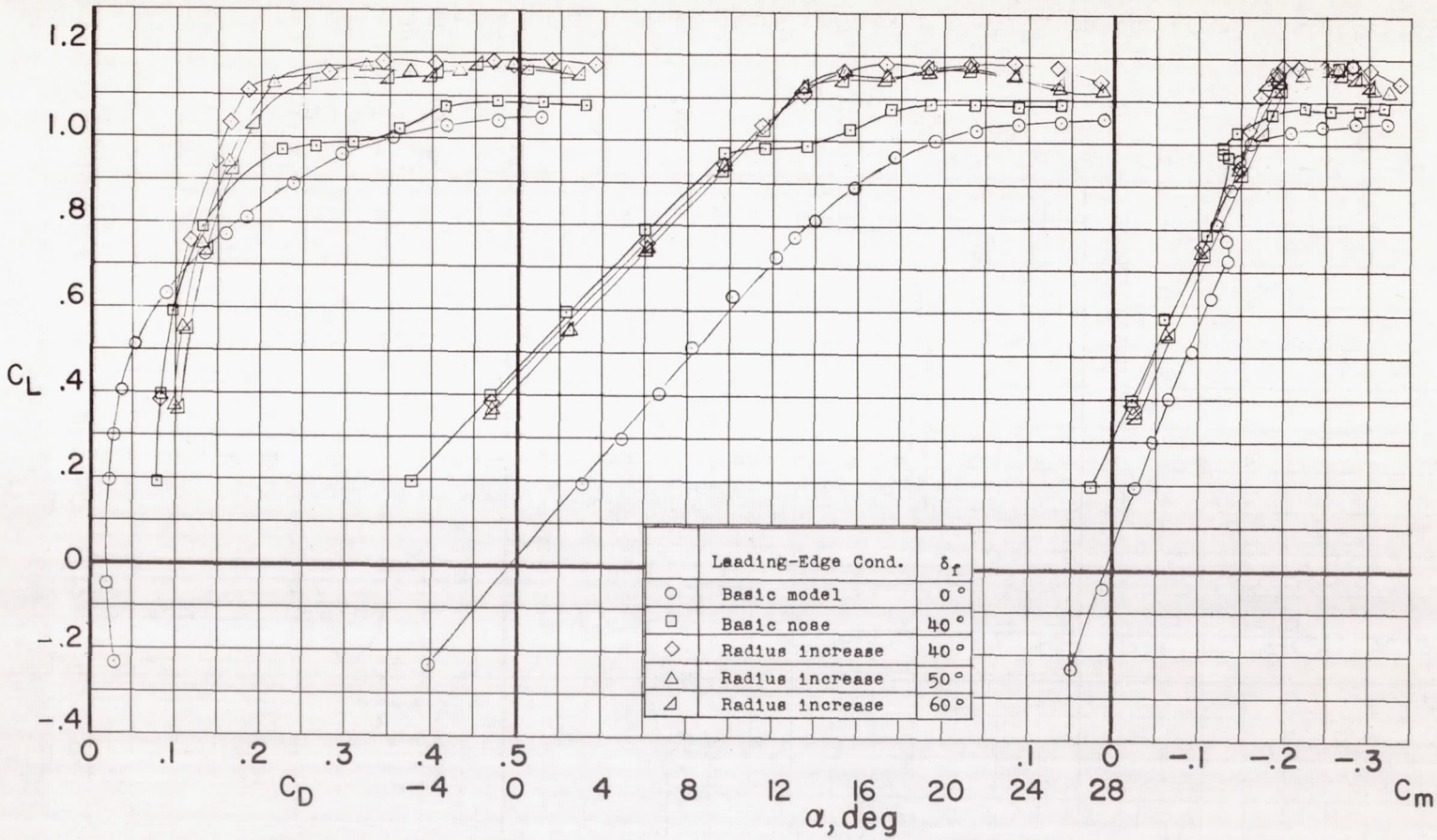

Figure 15.- Effect of trailing-edge-flap deflection with leading-edge radius increase installed.

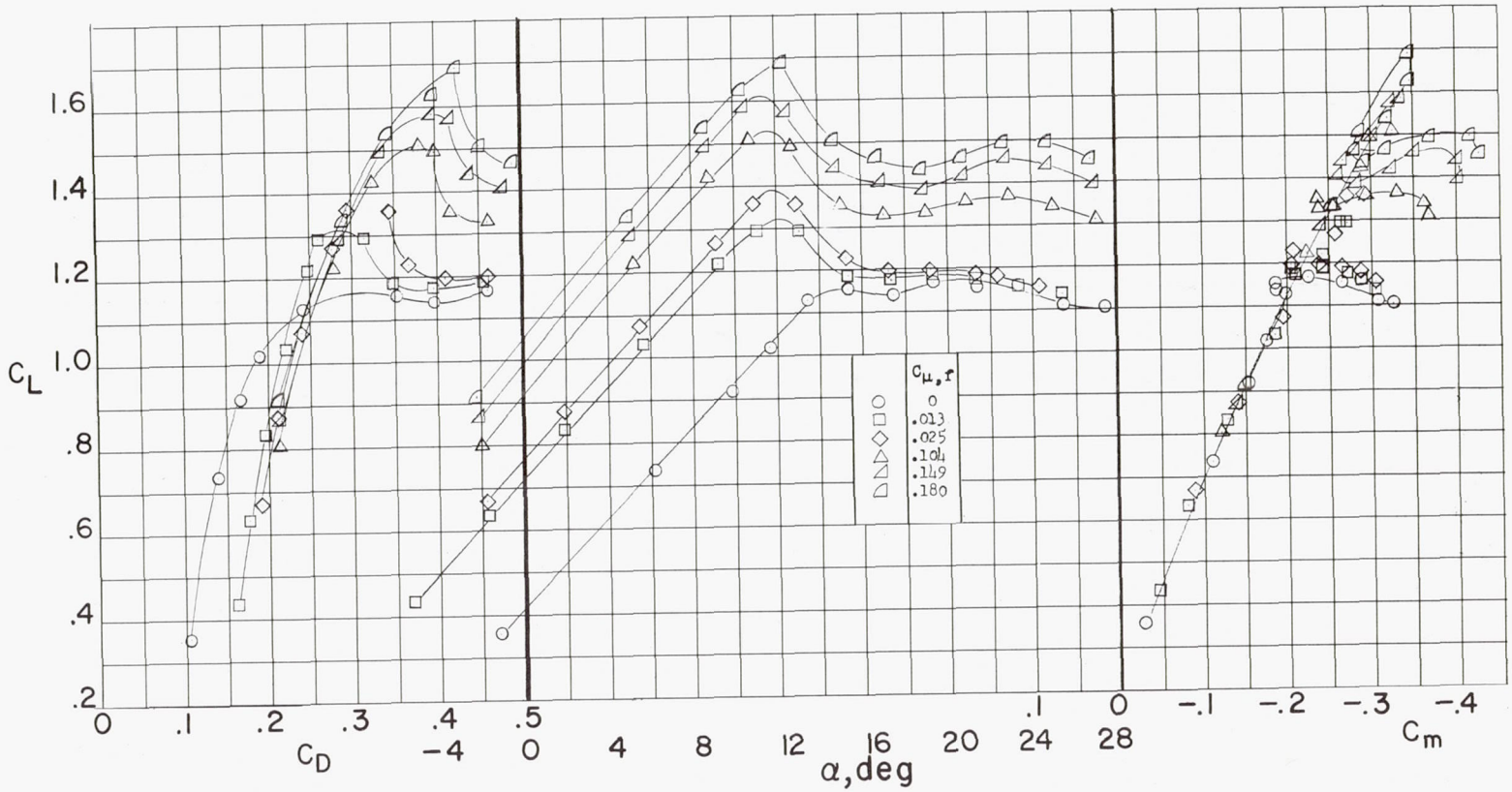

Figure 16.- Effect of flap-blowing type of boundary-layer control on the model characteristics with trailing-edge flaps deflected 60°. Leading-edge-radius increase.

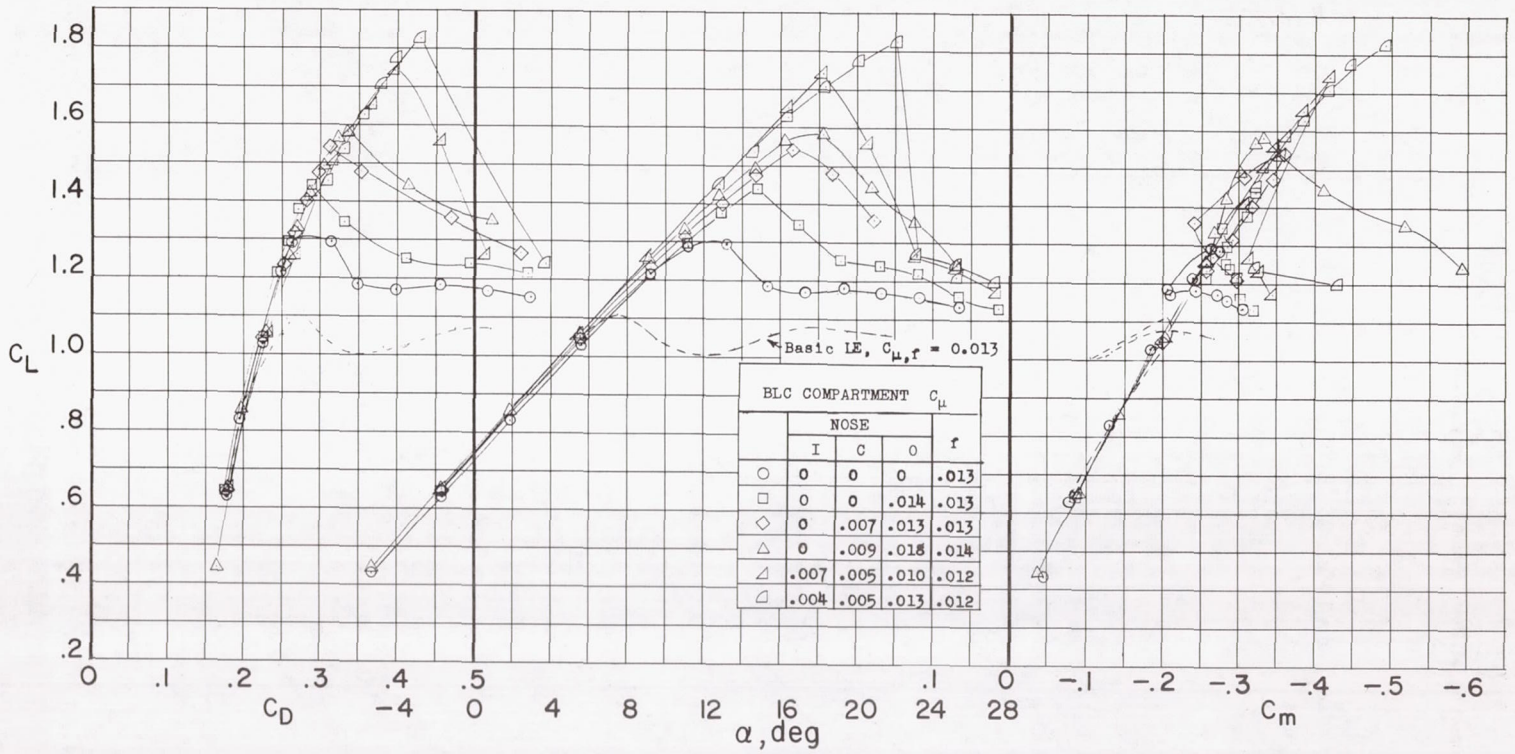

Figure 17.- Effect of a radius increase in conjunction with blowing over the leading edge and flap. $\delta_f = 60^\circ$.

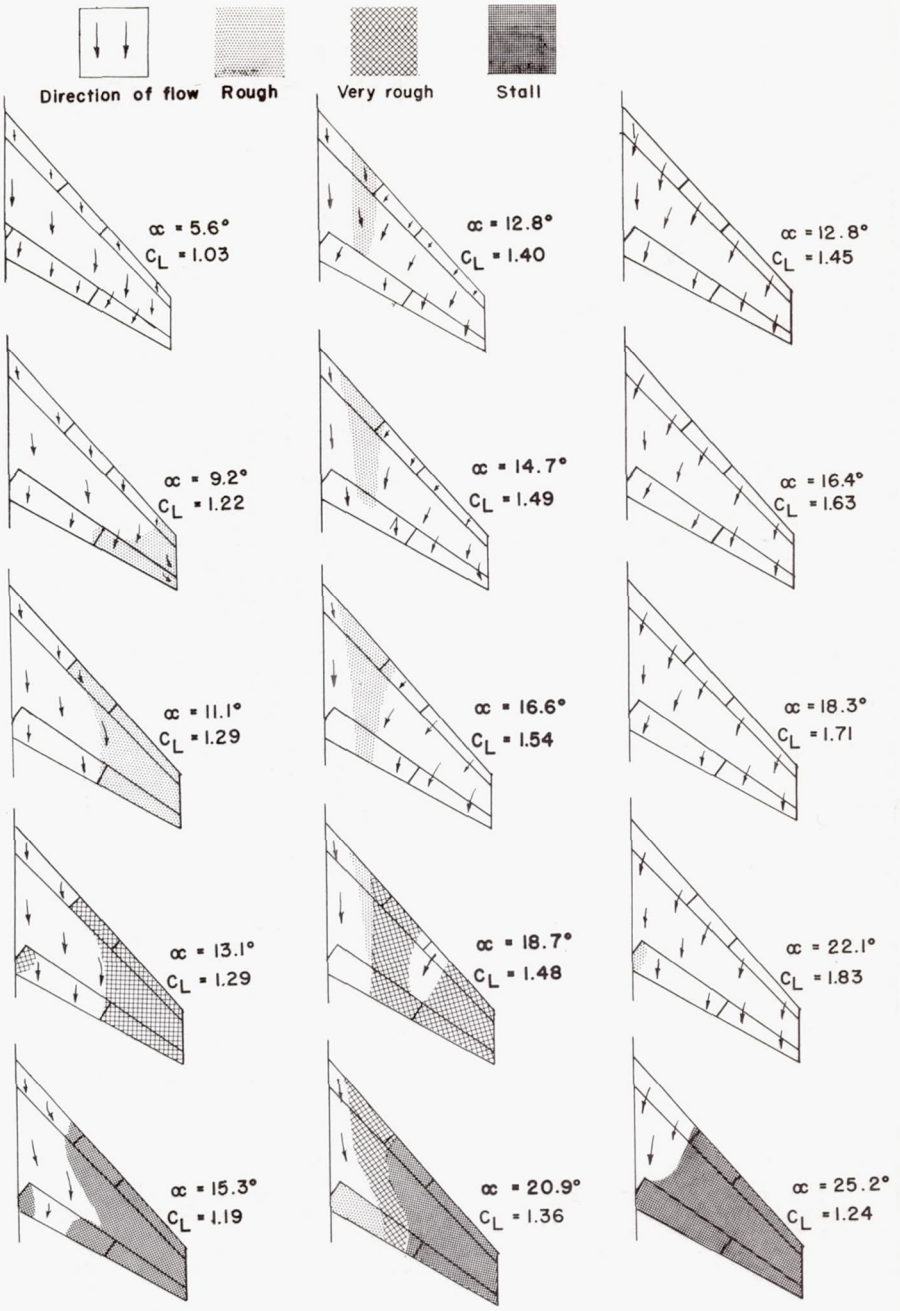

Leading edge			$C_{\mu,f}$
I	C	O	
0	0	0	.024

NOSE			$C_{\mu,f}$
I	C	O	
0	.007	.013	.024

NOSE			$C_{\mu,f}$
I	C	O	
.004	.005	.013	.024

Figure 18.- Wing flow patterns for model with nose with a radius increase and with flaps deflected 60°.

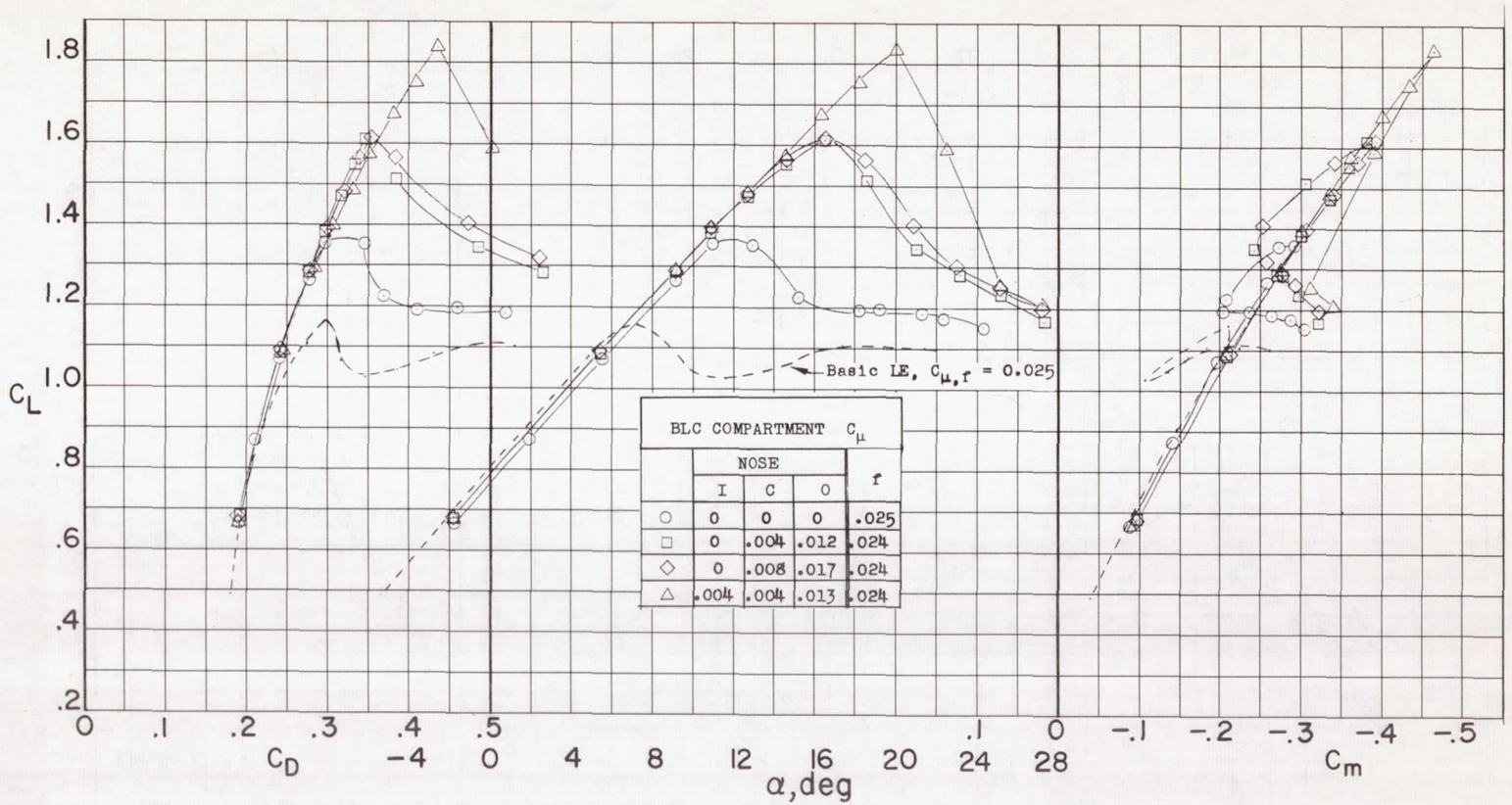

Figure 19.- Effect of a radius increase in conjunction with blowing over the leading edge and flap. $\delta_f = 60^\circ$.

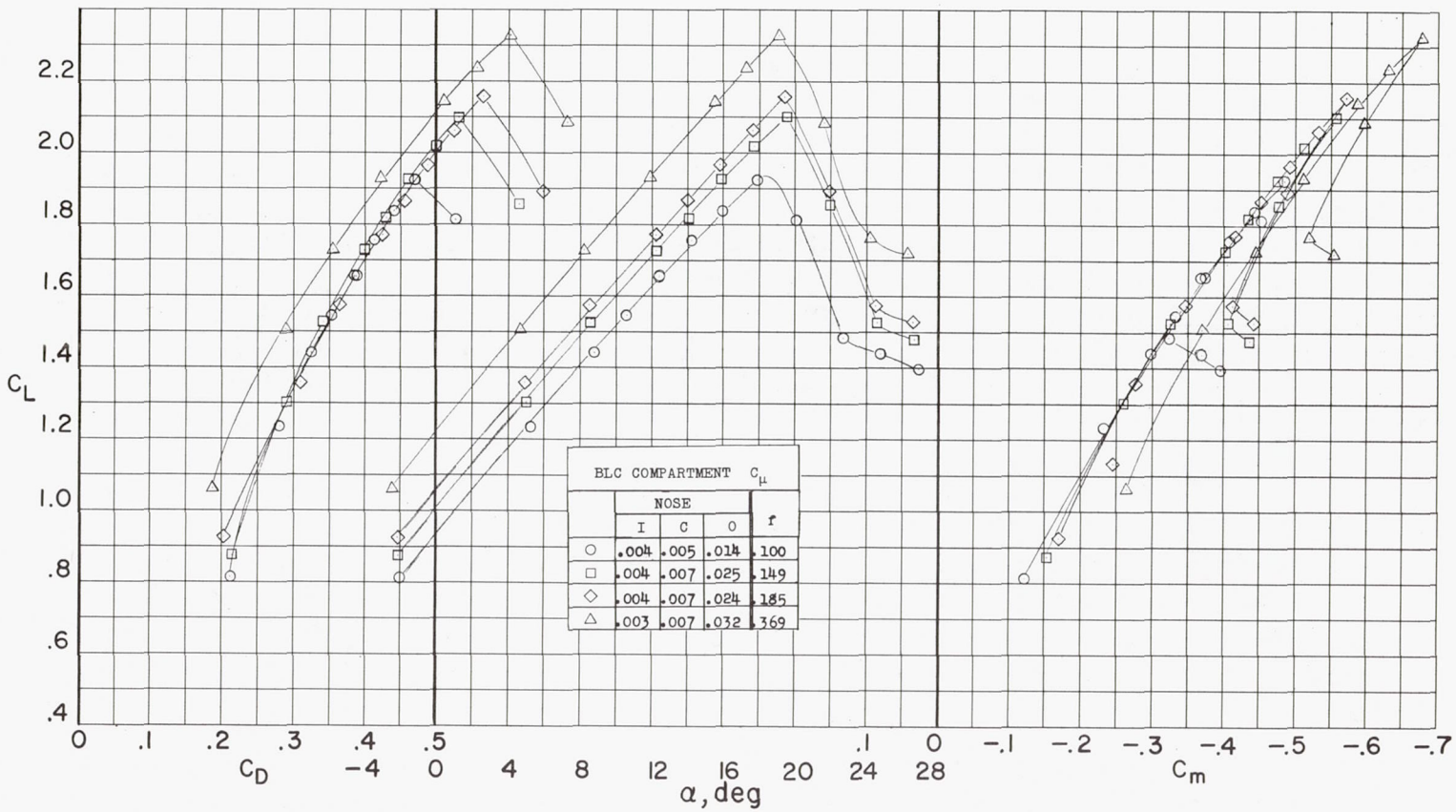

Figure 20.- Effect of a radius increase in conjunction with blowing over the leading edge and flap. $\delta_f = 60^\circ$.

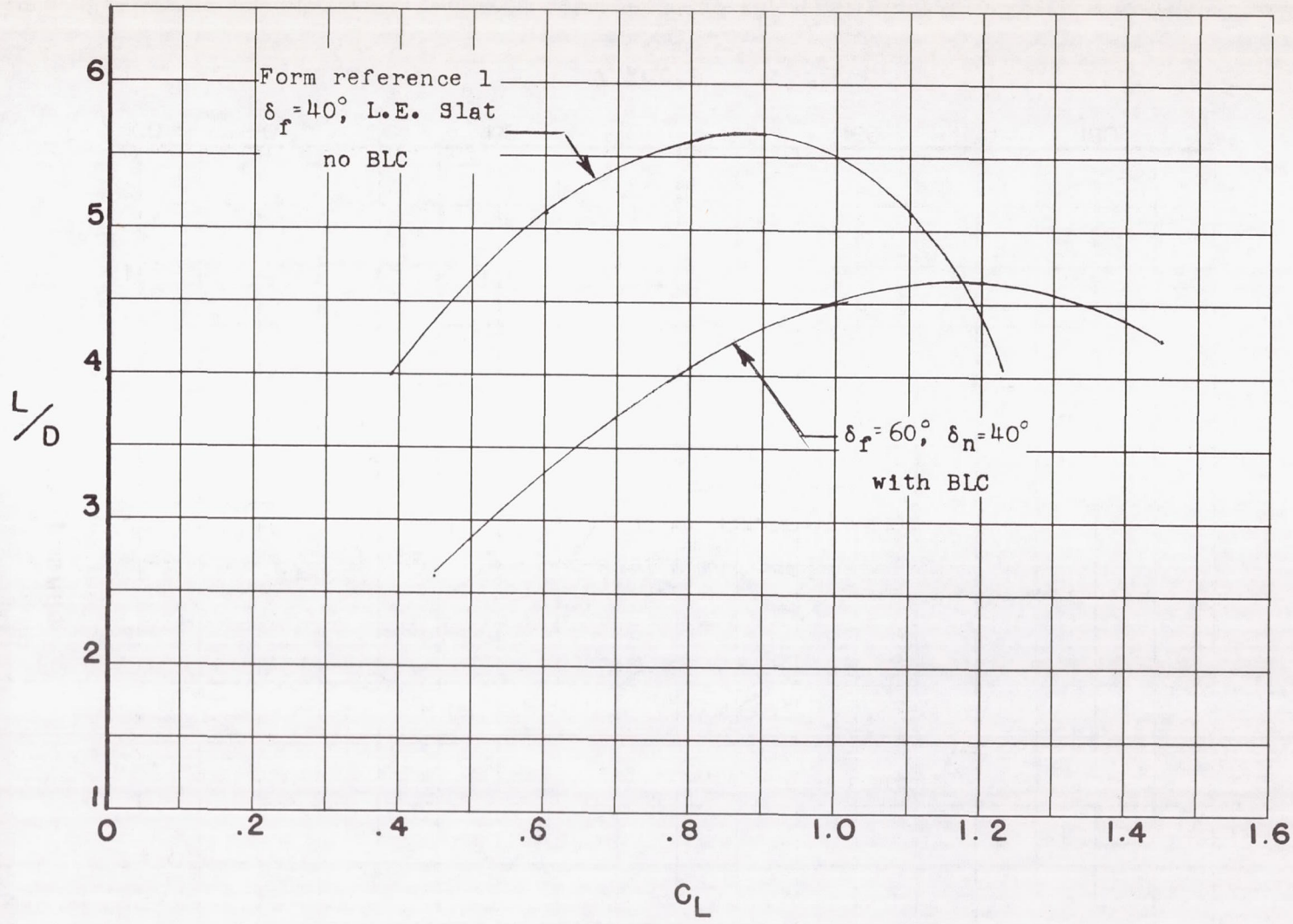

Figure 21.- Lift-drag ratios for the configuration with a boundary-layer control and for a typical configuration without a boundary-layer control.

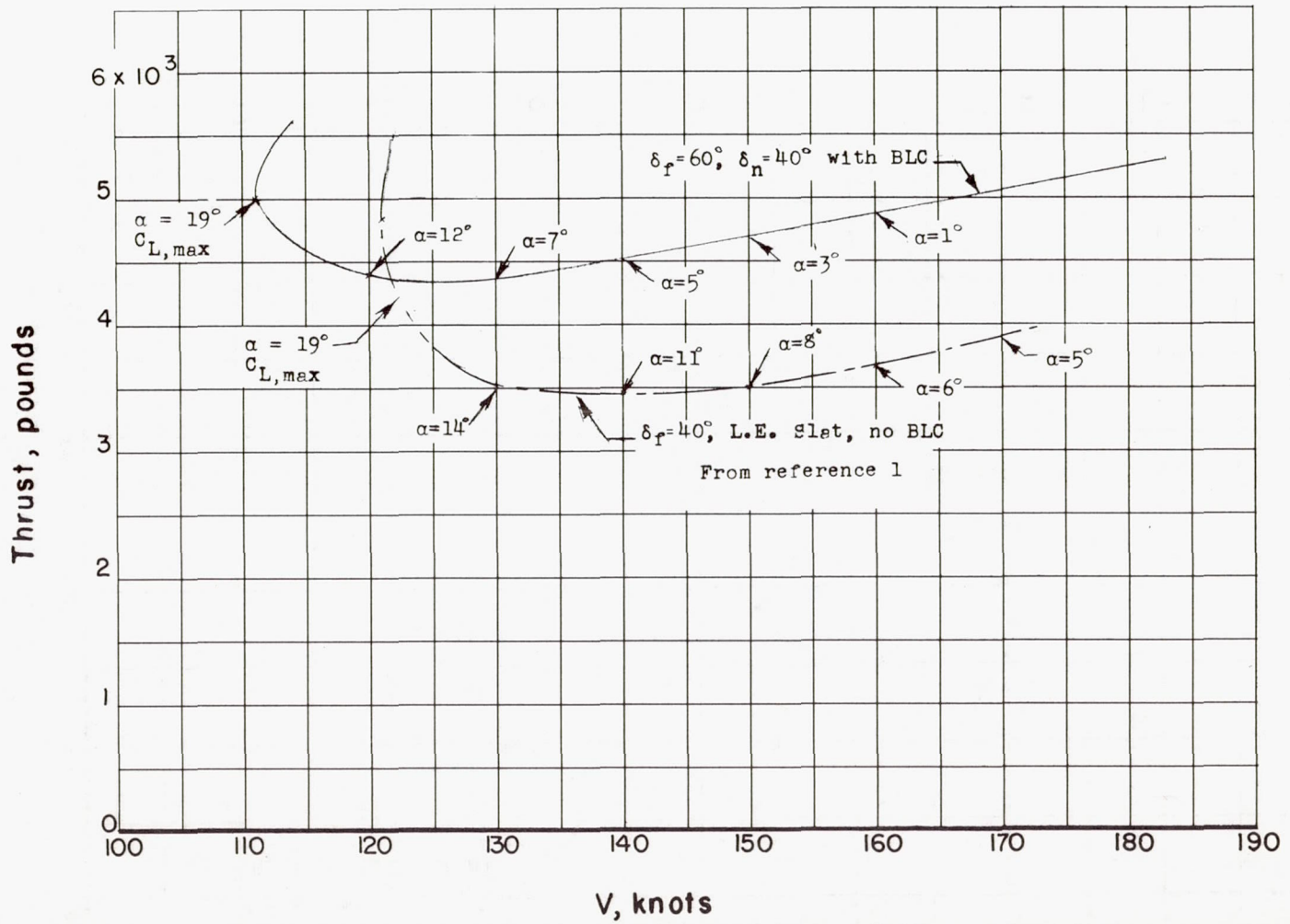

Figure 22.- Variation of thrust required with velocity for a configuration with a boundary-layer control with a given mass flow and pressure ratio and for a typical configuration without a boundary-layer control.

NACA - Langley Field, Va.